

1
2
3
4
5
6
7
8
9
10
11
12
13
14
15
16
17
18
19
20
21
22
23
24
25
26
27
28

Long-term visibility variation in Athens (1931-2013): A proxy for local and regional atmospheric aerosol loads

Dimitra Founda¹, Stelios Kazadzis^{2,1}, Nikolaos Mihalopoulos^{1,3}, Evangelos Gerasopoulos¹, Maria Lianou¹, Panagiotis I. Raptis¹

¹Institute for Environmental Research & Sustainable Development, National Observatory of Athens, Greece
²Physikalisch-Meteorologisches Observatorium Davos, World Radiation Center, Switzerland
³Department of Chemistry, University of Crete, Greece

Correspondence to: Dimitra Founda (founda@noa.gr)

Abstract. This study explores the inter-decadal variability and trends of surface horizontal visibility at the urban area of Athens from 1931 to 2013, using the historical archives of the National Observatory of Athens (NOA). A prominent deterioration of visibility in the city was detected, with the long-term linear trend amounting to $-2.8 \text{ kmdecade}^{-1}$ ($p < 0.001$), over the entire study period. This was not accompanied with any significant trend in relative humidity (RH) or precipitation over the same period. A slight recovery of visibility levels seems to be established in the recent decade (2004-2013). It was found that very good visibility ($>20 \text{ km}$) occurred at a frequency of 34% before the 1950s, while this percentage drops to just 2% during the decade 2004-2013. The rapid impairment of the visual air quality in Athens around the 1950s, points out to the increased levels of air pollution on a local and/or regional scale, related to high urbanization rates and/or increased anthropogenic emissions on a global scale at that period. Visibility was found to be negatively/positively correlated with relative humidity (RH)/wind speed, the correlation being statistically valid at certain periods. Wind regime and mainly wind direction and corresponding air masses origin were found to highly control visibility levels in Athens. The comparison of visibility variation in Athens and at a reference, non urban site on Crete island, revealed similar negative trends over the common period of observations. This suggests that apart local sources, visibility in Athens is highly determined by aerosol load of regional origin. Satellite derived aerosol optical depth (AOD) retrievals over Athens and surface measurements of PM_{10} confirmed the relation of visibility with aerosol load.

29 **1 Introduction**

30 Visibility is defined as the greatest distance at which a black object of suitable dimensions (located on the
31 ground) can be seen and recognized, when observed against the horizon sky during daylight, (WMO 1992).
32 Visibility represents one of the dominant features of the climate and landscape of an area. Although it is highly
33 affected by atmospheric circulation and the prevailing meteorological conditions, under clear sky conditions it is
34 mainly determined by the loading of atmospheric aerosols (Davis, 1991; Lee, 1994; van Beelen and van Delden,
35 2012; Doyle and Dorling, 2002; Singh and Dey, 2012), therefore, visibility can be considered as a strong
36 indicator of air quality over an area. Horizontal visibility has also been introduced in formulas for the estimation
37 of atmospheric turbidity parameters (e.g. in the Ångström atmospheric turbidity coefficients, Eltbaakh et al.,
38 2012).

39 Aerosols in the atmosphere contribute to light extinction by scattering and absorbing, thus reducing visibility
40 (Appel et al., 1985; Chan et al., 1999; Elias et al., 2009; Singh and Dey, 2012). The impact of particulate matter
41 on visibility depends on its physical (e.g. particle size distribution) and chemical properties (Dayan and Levy,
42 2005). In particular, visibility is inversely related to light extinction coefficient, which is determined by scattering
43 and absorption of light by gases and particles, the latter (e.g. sulphate and carbon containing particles) being the
44 main contributor (Malm, 1999; Hand et al., 2002; Baumer et al., 2008; Deng et al., 2011; Wang et al., 2012).
45 Sulphate and carbon containing particles play a major role in light extinction, while the role of relative humidity
46 (RH) on visibility is also important (Larson and Cass, 1989; Malm, 1999), as when RH reaches saturation values,
47 visibility deteriorates due to fog formation and the hygroscopic growth of SO_4^{2-} , NH_4^+ and NO_3^- particles (Tang,
48 1996; Singh and Dey, 2012). At local and regional level, wind speed and direction are also very important factors,
49 as they determine the transport and origin of air pollution.

50 Although the use of visibility as a viable atmospheric variable has been disputed by many researchers due to the
51 numerous biases related to observational procedures (Davis, 1991), visibility statistics have been increasingly
52 used as a surrogate for aerosol load (Zhao et al., 2011), especially since visibility records span quite long-term
53 periods. Today, there is a large number of studies that use visibility observations to investigate the spatial and
54 temporal variation of the optical properties of the atmosphere, mainly in relation to pollutant emissions and
55 aerosol load. These studies refer to global, regional and local scales. On a global scale, a decrease of clear sky
56 visibility over land from 1973 to 2007 is reported by Wang et al. (2009). This is interpreted in terms of aerosol
57 concentrations and its impact on incident solar irradiance. A significant decrease of visibility is observed over

58 Asia, South America, Australia and Africa (1973-2007), while over Europe visibility increased after the 1980s, as
59 a result of air pollution mitigation measures. Vautard et al. (2009) found a significant decrease in the frequency of
60 low visibility days in Europe after the 1980s, which is spatially and temporally correlated with SO₂ emissions.
61 Stjern et al. (2011) reported that emission reductions from 1983 to 2008 in the heavily industrialized area of
62 central Europe (the formerly called Black Triangle, BT, named from the triangle of the meeting borders of
63 Germany, Poland, and the Czech Republic) caused an increase in the horizontal visibility by 15 km, in contrast to
64 the clean area where visibility increased by only 2.5 km. Doyle and Dorling (2002) observed significant
65 improvement of visibility after the early 1970s at many sites in UK, attributed to anti-pollution measures, while
66 van Beelen and van Delden (2012) found that the proportion of days with high visibility (>19 km) almost doubled
67 since the early 1980s in the Netherlands. These findings for Europe are in line with the so called
68 dimming/brightening periods, referring to observed decreasing/increasing trends of surface solar radiation (SSR),
69 associated with relevant changes in anthropogenic emissions (e.g. Streets et al., 2006; Wild, 2009; Cermak et al.,
70 2010; Folini and Wild, 2011; Nabat et al., 2014).

71 In contrast to European areas, a tendency towards lower visibility is observed in developing countries (e.g. China,
72 South Korea, South Taiwan, India), where it is still difficult to control air pollution (Ghim et al., 2005; Che et al.,
73 2007; Wan et al., 2011; Singh and Dey, 2012; Wu et al., 2012). Along this line, Wu et al. (2012) found strong
74 correlation between AOD and visibility in China over the period 2000-2009, and an overall decreasing trend in
75 visibility (under sunny conditions) during the last 50 years. Singh and Dey (2012) correlated visibility in Delhi
76 with aerosol composition and reported a rapid decrease of visibility during 1980-2000, and stabilization
77 afterwards.

78 Urban environments are of particular interest, as air pollution from local sources is superimposed on regional
79 ones, strongly impacting visibility (Davis, 1991; Eidels-Dubovoi, 2002; Tsai et al., 2003, 2007; Dayan and Levy,
80 2005; Chang et al., 2009; Kim, 2015).

81 The present study explores the historical observations of visibility in Athens, which is the oldest time series of
82 visibility in Greece and, to our knowledge, one of the oldest, uninterrupted time series of visibility in the eastern
83 Mediterranean. The records are retrieved from the historical climatic archives of the National Observatory of
84 Athens (NOA) and span a period of more than 80 years (1931-2013). In the past, Carapiperis and Karapiperis
85 (1952) reported on the correlation between the visibility and the blue colour of the Attika sky, while
86 Kanellopoulou (1979) analysed visibility in Athens for the period 1931-1977 and reported a pronounced decrease
87 after the 1950s. Since then, there has been no other study to address changes in visibility, as well as the

88 factors behind these changes during the last 40 years, when significant changes occurred in Athens in terms of
89 urban expansion, traffic load, 2004 Olympic Games construction and the economic recession (starting in 2008).
90 The inter-decadal variability and long-term trends of visibility in Athens are presented in the study. The role of
91 meteorology and aerosol load (of local and regional origin) on the variability and trends of visibility are
92 investigated and discussed, while the relationship between visibility and aerosol load is investigated, through the
93 analysis of satellite AOD retrievals over Athens, but also surface measurements of PM₁₀ in Athens and Finokalia
94 station (Crete) over shorter periods.

95

96 **2 Study area and data**

97 **2.1 Study area**

98 Athens, the capital of Greece, is the main centre of commercial, financial, societal and cultural activities of the
99 country. The Greater Athens Area (GAA) (Fig. 1) extends beyond the administrative municipal city limits and
100 covers a surface of 433 km². The population of GAA is approximately 3.7 million (almost twice the population of
101 1961) and accounts for more than one third of the Greek population. The growth of the population was coupled
102 with a significant increase in the number of vehicles. Specifically, the number of private cars rose from 2% of
103 inhabitants in 1964 to 44% in 2008. The population growth and the increased number of automobiles have caused
104 traffic problems, increased anthropogenic emissions and degradation of air quality in the city. The complex
105 topography, consisting of relatively high mountains around GAA (Fig. 1), induces poor ventilation of the city.
106 Sea/land breezes appear along the NE - SW axis and play a dominant role in the accumulation of air pollutants
107 (Kalabokas et al., 1999a,b).

108 In order to compare our findings for Athens with a reference, remote site, the visibility records from the
109 Heraklion airport (HER) in Crete Island were used (Fig. 1). Heraklion is located about 330km south of Athens,
110 while its airport is 5km east of the city with no significant (or systematic) influence by the urban web.

111 **2.2 Climatic features of Athens**

112 Athens has a temperate climate with warm and dry summers and wet and mild winters, typical for eastern
113 Mediterranean. Table 1 presents monthly and annual normal values along with standard deviations of the daily
114 mean, maximum and minimum air temperature, precipitation amount and precipitation frequency (PF) (defined

115 as the number of days with total precipitation > 1mm, following WMO), relative humidity and wind speed in
116 Athens, based on the WMO reference period, 1971-2000. July and August are the warmest and driest months of
117 the year. The periods from May to September and from October to March represent the dry and wet periods of
118 the year respectively. Precipitation is sparse in summer (June- August), with the total amount averaging 20mm
119 and precipitation frequency averaging 3 days. Athens receives on average approximately 400 mm of rain per
120 year, corresponding to 43 rainy days (Table 1).

121 During summer, the area is dominated by anticyclonic circulation that enhances air temperature and intensifies
122 urban heat island. Athens has been experiencing a significant warming since the mid 1970's, more pronounced in
123 summer, which is the additive result of regional warming and gradual intensification of the urban heat island
124 (Founda, 2011; Founda et al., 2015). Strong northeasterly winds in summer, known from antiquity as 'Etesians',
125 induce a relief on air temperature and air pollution levels in the city.

126 Figure 2a presents the main sectors related to air masses origin in Athens, based on 10-yr climatology of daily air
127 trajectories, while Fig. 2b presents the seasonal variability of air masses origin according to the sectors defined in
128 Fig. 2a. The S (south) sector is linked to transport of air masses from arid areas of N Africa, frequently associated
129 with dust events that affect the eastern Mediterranean (Hamonou et al., 1999; Gkikas et al., 2015), the N (north)
130 sector accounts for Balkans and the main continental Europe, while the W (west) sector corresponds to SW
131 Europe and the W Mediterranean Basin. Note that air masses transport from the W sector is significantly blocked
132 by the high altitude mountain chain of Pindus (>2500m), which expands from North to South along the western
133 Greek mainland. Air masses origin was identified by applying a 4-day back-trajectory analysis, calculated daily
134 at 12:00 UT with the Hybrid Single-Particle Lagrangian Integrated Trajectory (HYSPLIT) model (version 4.9)
135 (Draxler et al., 2009).

136 On an annual basis, air masses from the N and NE sectors dominate, contributing by more than 60% and showing
137 profound seasonal variability (maximum in summer). Similar conclusions are drawn from surface wind
138 measurements, reported in Fig. 3. Winds from N-NE directions prevail in Athens at a frequency of nearly 38%
139 (Fig. 3). This sector is also associated with the occurrence of high wind speeds, as shown in the same figure. The
140 second most frequent surface winds correspond to S-SW directions (27%). The frequency of occurrence of this
141 sector has maximum during the intermediate seasons (spring and autumn) and is associated with the occurrence
142 of dust events from northern Africa and, in cases of light winds, with sea breezes from the Saronic Gulf (Fig. 1).

143 **2.3 Overview of air pollution in Athens**

144 A short introduction on the factors that diachronically control air pollution levels in Athens is presented here, to
145 facilitate the interpretation of visibility variations in terms of pollutants concentrations.

146 Air pollution in Athens has been systematically measured since the early 1970s. Road transport, domestic
147 combustion and industrial activity have been the main sources of air pollution in GAA throughout the years.
148 Downward trends of sulfur dioxide, black smoke, carbon monoxide and nitrogen oxides have been reported from
149 the mid 1980s to the late 1990s, attributed to several anti-pollution measures adopted by the state (e.g.
150 replacement of the old technology gasoline-powered private cars and the reduction of the sulfur content in diesel
151 oil) (Kalabokas et al., 1999a). Negative trends of NO₂, NO_x and O₃ from the mid 1980s to 2009 are also reported
152 in several urban stations (Mavroidis and Iliia, 2012).

153 Measurements of particulate matter (PM) had only occasionally been conducted in Athens before the EU
154 Directive (1999/30/EC) was launched, revealing increased concentrations of PM₁₀ (Hoek et al., 1997).
155 Chaloulakou et al. (2003) reported on PM₁₀ and PM_{2.5} at a single road traffic sampling location from 1999-2000
156 and underlined the contribution of local emission sources, mostly traffic, to the high levels of PM concentration.
157 Grivas et al. (2004) highlighted the significant vehicular contributions to PM₁₀ concentrations in Athens during
158 2001-2004 and quantified the exceedances of the annual limit set by the EU Directive.

159 Studying the contribution of local sources versus regional and the role of long-range transport over megacities of
160 the eastern Mediterranean, including GAA, Kanakidou et al. (2011) summarized that a significant number of PM
161 exceedances registered in Athens is associated with regional pollution sources or natural dust transport, clearly
162 highlighting the importance of regional transport processes. Theodosi et al. (2011) compared simultaneous mass
163 and chemical composition measurements of size segregated particulate matter (PM₁, PM_{2.5} and PM₁₀) at two
164 urban and a reference, non-urban background site, concluding that, during the warm season there is no significant
165 (actually <15%) difference in PM₁ between the urban and reference sites, while on the other hand, local
166 anthropogenic sources dominate during the cold season. Regarding the coarse fraction, a significant contribution
167 from soil was found in urban locations throughout the year, contributing significantly (up to 33%) to the local
168 PM₁₀ mass.

169 Regarding columnar aerosol load and using ground-based AOD measurements in Athens, Gerasopoulos et al.
170 (2011) showed that the greatest contribution (40%) to the annually averaged AOD, comes from regional sources
171 (namely the Istanbul metropolitan area, the extended areas of biomass burning around the north coast of the
172 Black Sea, power plants spread throughout the Balkans and the industrial area in the Po Valley). Additional

173 important contributors are dust from Africa (23%), whereas the rest of Europe contributes another 22%. Gkikas et
174 al. (2015) found good correlation between AOD_{550nm} and surface PM_{10} over the Mediterranean basin during desert
175 dust episodes (2000-2013) and reported higher intensity but lower frequency of such episodes over the central
176 and eastern Mediterranean. Additionally, Hatzianastassiou et al. (2009) found that local anthropogenic emissions
177 in GAA contribute by 15-30% to the total AOD, as derived from satellite-based AOD measurements.

178 Vrekoussis et al. (2013) reported on the improvement of air quality in Athens during the period 2008-2013, as a
179 result of the economic recession and the subsequent reduction in vehicle use and industrial activity. For the same
180 period, Paraskevopoulou et al. (2014) showed that the massive turn of Athens' population to wood burning for
181 residential heating purposes gave rise to smog episodes characterized by high PM spikes during nighttime in
182 winter. A longer-term (2008-2013) analysis of aerosol chemical composition and sources at a suburban site in
183 Athens by Paraskevopoulou et al. (2015) revealed that the area of Athens is now generally dominated by aged,
184 transported aerosols.

185 **2.4 Visibility observations in Athens**

186 The historical climatic record of the National Observatory of Athens (NOA) was used in this study. NOA is
187 located on the Hill of Nymphs (latitude: $37.97^{\circ}N$, longitude: $23.71^{\circ}E$, altitude: 107m, above sea level), at the
188 historical center of the city, near Acropolis. The location of the observations on the top of a hill ensures
189 unobstructed view towards all directions. Visibility observations have been conducted uninterruptedly at NOA at
190 least 3 times per day, since the late 1920's. Daily observations of visibility at 14:00 LST (LST= UT+ 2hrs), from
191 1931 to 2013 were used in the study. The time series is complete, with a very short gap of 6 days occurring in
192 December 1944, owed to political convulsion in the country at that period.

193 Visibility data at other stations (e.g. Heraklion, Crete) were extracted from the network of the Hellenic National
194 Meteorological Service (HNMS) and actually represent visibility observations at the airport station, initiated after
195 the mid 1950s. Meteorological data for Athens over the period 1931-2013, was also acquired from the historical
196 archives of NOA. Monthly, seasonal and annual mean values of visibility were derived from the daily
197 observations at 14:00 LST.

198 An empirical scale of visibility classes, as recommended by the World Meteorological Organization (WMO), has
199 been used for visibility observations at NOA (Table 2). Classes are defined based on the greatest distance at
200 which a predefined object can be seen and recognized with the naked eye. The procedure requires that an

201 operator scans the horizon for predetermined objects. In the case of Athens, some historical buildings in the city,
202 but also certain objects of the surrounding landscape unaltered over the years, (e.g. objects on the mountains or
203 islands of the Saronic Gulf, Fig. 1), were chosen to represent visibility classes and relevant distance ranges. The
204 procedure introduces inevitably some kind of subjectivity and bias in the measurements, related to individual
205 eyesight of different operators. It is assumed however, that the execution of visibility observations by different
206 operators over the years could have possibly had a compensating effect and an overall reduction of biases. More
207 details about the possible errors and validity of visibility observations have been thoroughly discussed by Davis
208 (1991).

209 The use of the WMO scale introduces a further uncertainty on visibility observations, associated with the
210 amplitude of visibility ranges corresponding to each visibility class. Information on the use of WMO scale and
211 relative uncertainties, as well as the followed procedure for averaging daily visibility observations is provided in
212 Supplementary materials.

213 **2.5 Aerosol data used in the study**

214 Long time series of atmospheric pollution measurements in Athens and the selected reference site would enable
215 drawing relationships between visibility and aerosols and would provide evidence for the origin (regional or local)
216 of atmospheric pollution in Athens and its impact on long-term visibility variations. Given that such time series
217 are missing, we used shorter time series of aerosol measurements for a direct comparison between visibility and
218 atmospheric pollution in Athens.

219 In an effort to explore the relationship between visibility and AOD over Athens, we used the Terra/Modis AOD
220 at 550nm, available since 2000. NASA's Terra satellite is sun synchronous and near polar-orbiting, with a
221 circular orbit of 705 km above sea level. MODIS is capable of scanning 36 spectral bands across a 2330 km
222 swath. MODIS aerosol products were used in order to analyze the temporal and spatial variability of
223 aerosols over the wide area of interest. In this study, we used daily level-2 collection 5.1 MODIS/Terra AOD at
224 550 nm. Daily overpass data for the specific area was extracted at a spatial resolution of 50x50 km². Previous
225 studies have shown that such spatial resolution product ensures sufficient daily measurements without losing out
226 to the higher spatial resolution and hence provides a better opportunity of correctly viewing the atmospheric
227 aerosol load (Ichoku et al., 2002). The overpass time is 09:35 ± 45 min UT.

228 In addition, in order to further examine long-term satellite based AODseries in the area, we used the longest
229 satellite timeseries available from the Advanced Very High Resolution Radiometer (AVHRR). AOD retrievals
230 PATMOS-x AVHRR level-2b channel 1 (630nm) provide data over global oceans at high spatial resolution (0.1°
231 $\times 0.1^\circ$), for one overpass per day. Data used were downloaded from NOAA Climate Data Record (CDR) version
232 2 of aerosol optical thickness (Zhao and Chan, 2014) and cover the period from August 1981 to December 2009.
233 Version 2 dataset has enhanced cloud screening and retrieves AOD only over non-glint water surface, which has
234 less uncertainties of surface reflectance. AVHRR instrument is not designated for retrieving AOD, thus its
235 product embodies a large variety of uncertainties, including radiance calibration, systematic changes in single
236 scattering albedo and ocean reflectance (Mishchenko et al., 2007). Current dataset radiances have been
237 recalibrated using more accurate MODIS data (Chan et al., 2013). Smirnov et al. (2006) compared 38 days of
238 shipborne measurements with a MICROTOPS-II, on a cruise in Atlantic Ocean to AVHRR AOD retrievals and
239 found an average 0.05 overestimation of satellite data, with correlation coefficient equal to 0.95. We used
240 dailyoverpass data at the region around Athens (latitude: 37.5° - 38.2° E, longitude: 23.2° - 24.4° N) which included
241 72 active (ocean) grid-points. The above region was selected based on data availability on each grid with the
242 distance up to 70 km from the visibility observing site.

243 Surface PM_{10} measurements in Athens were also used to verify the relationship between visibility and particulate
244 pollution from surface measurements. It is well known that desert dust plumes are often transported in altitude
245 over the Mediterranean (e.g. Hamonou et al., 1999; Gkikas et al., 2015) and a portion of surface PM exceedances
246 in Athens is associated with natural dust transport (Kanakidou et al., 2011). The analysis was based on a short
247 dataset of PM_{10} at two stations in Athens (Aristotelous and Maroussi), covering the period 2008-2012. Aristotelous
248 is an urban street station in the center of the city and Maroussi is a suburban station, at a distance of about 15 km
249 to the North of NOA.

250 Finally, a dataset of PM_{10} measurements at a reference station in Crete (Finokalia station), covering the period
251 2005-2014 was used, for the detection of any trends, representative of regional atmospheric pollution trends. The
252 Finokalia station (35.240° N, 25.600° E) is located on the northern coast of Crete (Greece), at a distance of
253 approximately 320 km to the south of Athens. There is no significant human activity within an area of nearly 15
254 km around the station, mainly characterized by scarce vegetation. The closest large urban area is the city of
255 Heraklion (HER), (see map. of Fig. 1) with 150 000 inhabitants, and located 50 km West from Finokalia.
256 Aerosols at the site are mainly transported from the southern-eastern Europe and northern Africa, and to a lesser
257 extent from central and western Europe (Kouvarakis et al., 2000).

259 **3 Results**

260 **3.1 Inter-decadal variation and trends of visibility**

261 Figure 4 displays the long-term development of the annual visibility in Athens from 1931 to 2013. The population
262 growth in the city of Athens over the same period is also shown, while the figure also displays the long-term
263 variability of the relative humidity in Athens (which is discussed below). It is obvious that the annual visibility in
264 Athens has undergone a very strong and almost continuous decline over the past 80 years, in coincidence with the
265 increase in population. The long-term linear trend over the entire study period was found to be equal to -0.28 km yr^{-1}
266 (or $-2.8 \text{ km decade}^{-1}$, $p < 0.001$). However, this trend is not constant throughout the entire study period. The
267 following three sub-periods, corresponding to different trends, are visually discerned in Fig. 4 (also confirmed by
268 sensitivity tests): (a) 1931-1948, (b) 1949-2003 and (c) 2004-2013. Visibility levels are remarkably higher in the
269 first sub-period, varying around 25 km. A slight negative trend is observed during this period (-0.07 km yr^{-1}). In
270 the late 1940s, visibility experienced a striking and abrupt decrease at the time of first population burst, which
271 was then followed by a progressive deterioration, at least until the early 2000s. In this second sub-period (1949-
272 2003) visibility decreases at a rate of -0.23 km yr^{-1} (or $-2.3 \text{ km decade}^{-1}$, $p < 0.001$). A tendency of stabilization or
273 even recovery seems to be established during the more recent decade 2004-2013, when visibility exhibits a slight
274 increasing trend ($+0.07 \text{ km yr}^{-1}$). A detailed discussion on the observed trends and their links to air pollution is
275 presented in section 3.5.

276 **3.2 Frequency distribution of visibility ranges**

277 The separation of the time series into three sub-periods was indicated by the fact that they represent periods of
278 changing trends. In the following, the much longer middle sub-period (1949-2003) was further separated into two
279 parts (1949-1975 and 1976-2003) as it corresponds to substantially different visibility conditions. Figure 5
280 illustrates the frequency of occurrence of different visibility ranges as described in Table 2 for different sub-
281 periods.

282 In the first sub-period (1931-1948), visibility values are almost equally distributed between the ranges of 10-20
283 km and 20-50 km, at frequencies of approximately 35%. Very high visibility ($>50 \text{ km}$) accounts for a considerable
284 portion ($\sim 9 \%$) of this sub-period and poor visibility ($< 2 \text{ km}$) corresponds cumulatively to only 2%. The frequency

285 of visibility lower than 1 km is very low (0.4%), while visibility lower than 500m occurred only in 9 cases.
286 Cumulatively, visibility exceeded 10 km at a frequency of approximately 80% during this period.

287 A progressive shift of frequency distribution towards lower visibility categories is observed in the next sub-
288 periods. In particular, the frequency of very good visibility (20-50 km) drops to 13% and 6% for the periods
289 1949-1975 and 1976-2003 respectively, while the most frequent visibility range is 10-20 km (44%) during 1949-
290 1975 and 4-10 km (41%) during 1976-2003. The frequency of visibility >50km is almost negligible (~ 1% during
291 1949-1975) and the frequency of poor visibility (<2 km) amounts cumulatively to 9 % and ~ 1% for 1949-1975
292 and 1976-2003 respectively. Lower than 500m visibility was observed only in 2 cases during 1949-1975 and in 10
293 cases during 1976-2003. Cumulatively, the percentage of days with visibility exceeding 10 km drops to 58% and
294 29% for the periods 1949-1975 and 1976-2003 respectively.

295 The frequency distribution changes dramatically during the most recent period (2004-2013). In particular,
296 although visibility range of 4-10 km remains the most frequent (30%), as in the sub-period 1976-2003, almost
297 similar frequency (~28%) is also observed in the range of 2-4 km. The frequency of poor visibility (<2km) rises to
298 approximately 25%, with a substantial percentage (5.6%) accounting for visibility lower than 1 km and 0.46 %
299 lower than 500 m. Overall, visibility did not exceed 4 km for half of the days of the year during 2004-2013. The
300 percentage of days with visibility > 10 km is 18%, while frequency of very good visibility (>20 km) amounts to
301 just 2%. No case of visibility > 50 km was observed in this last sub-period.

302 **3.3 Seasonal variation of visibility**

303 Since visibility is influenced by the prevailing meteorological conditions (Davis 1991; Sloane 1982), it is
304 expected to exhibit a seasonal variability, depending on the intra-annual variability of climatic conditions at the
305 study area. Mean monthly values of visibility were calculated for the sub-periods 1931-1948, 1949-1975, 1976-
306 2003 and 2004-2013. Figure 6 (a-d) presents the mean monthly values of visibility in Athens over each sub-
307 period, normalized with the value of the month with the highest visibility. In the same plot, the mean monthly
308 values of relative humidity (RH) coinciding visibility observations at 14:00 LST over each sub-period are also
309 shown. It is noteworthy that RH at NOA does not exhibit any significant trend over the years (as already shown
310 in Fig. 4) and its monthly distribution remains almost unaltered in all sub-periods. As it results from Fig. 6 (a-d),
311 visibility exhibits a seasonal cycle in all sub-periods, with better visibility occurring in the warm and dry months
312 of the year. Although seasonality is observed in all sub-periods, the pattern is more evident and robust in the first
313 sub-period (Fig. 6a), with much higher visibility values (up to 40%) in the warm and dry months. The pattern of

314 visibility in this period is almost a mirror image of the pattern of RH and reflects the influence of RH on visibility
315 and the anti-correlation between these two variables. The lowest values of RH correspond to July and August
316 (mean value of RH ~35% at 14:00 LST) and this probably results in visibilityimprovement. Moreover, strong
317 northeasterly winds that prevail in eastern Greece during these monthsenhance ventilation and induce drier
318 conditions in the city, therefore improving visibility.

319 The distinct seasonal cyclein visibility of the first sub-period changed in the following sub-periods (Fig. 6, b-
320 d).Although the warm and drier months always correspond to higher visibility levels, seasonality is noticeably
321 attenuated and visibility differences between the warm and cold period are much lower. This possibly implies a
322 weakening of the influence of meteorological conditions, as a result of (or in combination with) the stronger
323 effect of air pollution on the visual air quality of the city.

324 The minimum of visibility is constantly observed in March during all sub-periods. Indeed, March is a month of
325 transitional season and thus bears higher values of RH compared to summer months (mean value of RH at 14.00
326 LST > 50% and mean daily value 67% in March). Additionally, March is a month of the growing season, with
327 enhanced pollen and biogenic aerosol emissions which is a known factor for visibility impairment (e.g. Kim,
328 2007). Increased frequency of dust outbreaks from northern Africa in spring, influence extensively the area of
329 eastern Mediterranean (Hamonou et al., 1999; Gerasopoulos et al., 2005, 2011; Gkikas et al., 2015) and thus
330 constitute a major factor for visibility impairment during spring months. Léon et al (1999) reported that ~ 40% of
331 the days with high aerosol optical depth at 865 nm ($AOD_{865nm} > 0.18$) over Thessaloniki (Greece) were associated
332 with African dust transport events, all observed in the period March - July, while Dayan and Levy (2005) found
333 higher PM_{10} values and lower visibility levels during spring in Tel Aviv, associated with the frequent passage of
334 cyclones that cause natural dust outbreaks.

335 **3.4 Visibility and meteorological conditions**

336 The impact of meteorological conditions on visibility has been investigated by different researchers using
337 different approaches, as for instance the classification of synoptic circulation patterns (Sloane, 1982; Davis, 1991;
338 Dayan and Levy, 2005), the application of correction factors on extinction coefficient to account for RH effect
339 (Che et al., 2007), the estimation of correlation coefficients between visibility and meteorological variables
340 (Deng et al., 2011), or simply the comparison of diurnal/seasonal cycles and temporal trends of visibility with the
341 relevant cycles and trends of meteorological variables (van Beelen and van Delden, 2012). Sloane (1982)
342 reported that periods with exceptionally maxima or minima of visual air quality were related (apart from sulphate

emissions) to favourable synoptic circulation patterns. Studying visibility in Tel Aviv (Israel), Dayan and Levy (2005) reported a strong dependence of visibility levels on meteorological conditions, synoptic weather patterns and airmass origin, with the highest mean values occurring in summer, related to the persistent nature of the summer synoptic weather patterns in the eastern Mediterranean. Deng et al. (2011) found that RH and wind speed were significantly correlated with visibility at an urban area of China, while Ghim et al. (2006) showed a considerable decrease in visibility in South Korea, despite the observed simultaneous decrease of RH levels. The relationship and possible impact of different meteorological parameters such as precipitation, RH, wind speed and wind direction on visibility in Athens is discussed below.

3.4.1 Visibility and precipitation

Precipitation is associated with scavenging of atmospheric particles (e.g. Remoudaki et al., 1991a; 1991b), possibly resulting in improvement of visibility. The precipitation frequency in particular, was found to control seasonal variability of the total atmospheric deposition of lead in western Mediterranean (Remoudaki et al., 1991b). Rainy days, on the other hand, are associated with increased relative humidity, resulting in reduction of visibility. A plot illustrating the long-term variability of the annual precipitation amount and precipitation frequency (PF) at NOA from 1931-2013 was created, for the detection of any significant temporal trends (Fig. 7). As it results from the figure, no long-term trend is observed in the annual precipitation at NOA from 1931-2013, which could have had an effect on long-term trends of visibility. Precipitation frequency, on the other hand, exhibits an overall negative trend over the same period ($-1.1 \text{ days decade}^{-1}$) which is not constant throughout the time series. Specifically, PF decreases from the late 1960s to the late 1980s, while it presents an increasing tendency after 1990 ($+1.3 \text{ days decade}^{-1}$). The correlation coefficient between annual visibility and PF was found to be positive only during the period from the early 1970s to the late 1980s ($+0.45$, $p < 0.05$). A negative correlation coefficient was found in the post 1990 period (-0.21), not statistically significant.

Subsets of data were also produced for the creation of additional visibility time series, accounting for precipitation influence. Figure 8 presents visibility variability during the wet (October-March) and dry (May-September) period of the year, along with the annual values. Lower values during the rainy and cold period of the year are most probably associated with higher values of relative humidity, resulting in the reduction of visibility. Despite the differences between the time series in Fig. 8, the overall tendency is similar, thus not affecting the validity of our conclusions regarding the long-term visibility impairment in Athens. Additional plots, created from subsets of 'rain' and 'no rain' days are provided in Supplementary materials (Fig. S4).

372 3.4.2 Correlation between visibility and other meteorological parameters (RH, wind)

373 Figure 9 presents the running correlation coefficient (15-yrs window) between visibility and relative humidity at
374 NOA, over the period 1931-2013. As expected, the correlation coefficient between visibility and RH is negative,
375 indicating the anti-correlation between these two variables. High RH enhances water uptake by airborne particles,
376 leading to higher light scattering and thus, visibility impairment. Actually, when RH exceeds a threshold level
377 (e.g. > 70%), some inorganic salts, such as ammonium, sulfate and nitrate, undergo sudden phase transitions from
378 solid particles to solution droplets and become responsible for visibility impairment, as compared to other
379 particles that do not uptake water (Malm, 1999).

380 Following Fig. 9, the negative correlation between RH and visibility is statistically significant ($p < 0.01$) almost
381 over the entire study period. However, a progressive weakening of the correlation coefficient with time is
382 observed, indicating a less strong correlation between the two variables over the years. Stronger anti-correlation
383 is found until the early 1970s, followed by lower (still significant) values until the late 1970s. The progressive
384 weakening of the correlation between RH and visibility in Athens, possibly suggests a progressive weakening or
385 mask of RH influence on visibility, compared to the effect of other factors such as atmospheric pollution
386 (although the influence of RH is enhanced by the presence of certain hygroscopic particles). On the contrary, the
387 impact of surface wind speed on visibility seems to be stronger during the late part of the time series (Fig. 9).
388 Higher wind speeds in this case (positive correlation) are related to the dispersion of air pollutants and the more
389 efficient city ventilation. In other cases, wind speed is also used as a proxy for long-range transport, but then a
390 negative correlation would be expected. Lower values of the coefficient in the early part of the time series
391 possibly demonstrate that the lack of pollutants at that period detracts from the importance of ventilation. The
392 correlation coefficient increases progressively over the years. The rate of increase is higher after the mid 1980s,
393 when correlation becomes statistically significant ($p < 0.01$). Similar values of correlation coefficient (~ -0.29)
394 between light extinction coefficient and wind speed are reported by Deng et al. (2011) in China.

395 Apart from wind speed, visibility was also found to be sensitive to wind direction. A distinct variability of
396 visibility with wind direction is observed in Fig. 10, for all sub-periods. Lower values of visibility are related to
397 southerly winds, as they bring either dust from Sahara or warmer and more humid air masses from the sea (see
398 also Figs 1, 2b). Southeasterly winds are, in general, weak winds (see Fig. 3), while southwesterly winds are
399 associated with sea breezes from the Saronic Gulf (Fig. 1). In general, sea breezes and calm wind conditions
400 favor the accumulation of pollutants and the formation of secondary aerosols and photochemical smog in Athens

401 (Colbeck et al., 2002), thus reducing visibility. A number of S/SW events are also associated with strong wind
402 speeds occurring during Sahara dust outbreaks, which enrich Athens atmosphere with dust particles that decrease
403 visibility (Figs 2, 3). As it results from Fig. 10, the highest visibility occurs under northwesterly winds and this is
404 robust for all sub-periods. An explanation for this, is that air masses originated from northwesterly directions are
405 much drier as they have lost water vapor after passing over the high mountainous basin of the Greek mainland
406 (e.g. Pindos mountain), while air pollution is also blocked within the boundary layer by the mountain chain.

407 **3.5 Air pollution and urbanization relations to visibility**

408 In this section, we attempt to interpret the observed inter-decadal variability and trends of visibility in Athens, in
409 terms of air pollution. As already shown in Fig. 4, the pre-1950 period is characterized by considerably higher
410 visibility levels in Athens. From then on, visibility experienced a rapid decrease, followed by a smoother but
411 continuous decreasing trend until the early 2000s. The period after 1950 signifies the post World War II epoch
412 but also coincides with the end of a civil war in Greece (1946-1949), which was followed by an important
413 urbanization wave in Athens (Maloutas, 2003). This is in line with the rapid growth of Athens' population, as
414 illustrated in Fig. 4. The greatest rate of population increase is observed between 1950 and 1960, when
415 population in Athens almost doubled. The population growth was associated with a significant increase of
416 construction in the city. But apart from the intense urbanization in Athens, this period is also characterized by the
417 most prominent increase of anthropogenic emissions on a global and European scale (e.g. Mylona, 1996; van
418 Aardenee et al., 2001, Vestreng et al., 2007,2009).

419 Are the changes in visibility in Athens due to local factors or can they be considered representative of a more
420 extensive area? To answer this question, the Athens visibility record was compared with visibility at a reference,
421 non urban station. From the available stations in Greece disposing long-term visibility observations, we chose the
422 station at Heraklion airport (HER) in Crete Island (Fig. 1). Actually, both sites, NOA and HER, are exposed, most
423 of the year, to air masses of similar origin (from north and northeasterly directions) travelling over the Aegean
424 Sea, in contrast to other sites of the country that are strongly affected by the mountainous volumes of the Greek
425 mainland. Visibility observations at HER are available since the mid 1950s. Figure 11 presents the long-term
426 variation of the annual averages of visibility at HER along with the annual visibility at NOA. Linear trends of
427 the time series for their common period (1956-2009) are also shown in the figure. The time series were found
428 significantly correlated (correlation coefficient > 0.88, $p < 0.05$).

429 According to Fig. 11, visibility levels at urban NOA are constantly lower by a few km (~ 7 km) compared to the
430 background station, HER. It is remarkable that, during the first two decades of parallel observations, both curves
431 show significant covariance, easily realized from the peaks in 1959, 1966 and 1970 and the minima in 1963 and
432 1973, suggesting the impact of large scale phenomena (for instance, volcanic eruptions in 1963) on the
433 modulation of visibility levels. A prominent feature in Fig. 11 is that, the background visibility at the reference
434 site has also been on a downward route since the mid 1950s, in accordance with the observed decreasing trend of
435 visibility in Athens. As already stated, the beginning of the 1950s corresponds to a period with significant
436 increase of emissions in Europe. European emissions of SO₂ in particular, increased almost at a constant rate
437 during the first half of the 20th century, while they experienced a quite abrupt increase in the 1950s (Mylona,
438 1996; van Aardenne et al., 2001; Vestreng et al., 2007). Figure 11 includes the historical development of SO₂ and
439 NO₂ emissions in Europe since 1930, as reported by Vestreng et al. (2007) and Vestreng et al. (2009)
440 respectively. A slow and constant increase of SO₂ emissions is observed until the 1950s (although the emissions
441 decreased during the World War II), related to the increased energy demand and use of solid fuels. A sharp
442 increase in sulphur emissions takes place afterwards, as a result of ongoing energy demand and availability of
443 liquid fuels (Vestreng et al., 2007), and in the late 1970s sulphur emissions were higher by a factor of nearly 2.5,
444 compared to the 1950's levels, exceeding 50 Tg SO₂. After a short stabilization in the 1980s, a sudden reduction
445 in sulphur emissions takes place (most prominent after 1990) which in the 2000s almost correspond to the levels
446 of 1930. Historical development of NO_x emissions in Europe exhibits a similar pattern (Fig. 11), with pronounced
447 increase in emissions from 1950 to 1980, a tendency of stabilization between 1980 and 1990 and a decline
448 thereafter. The plot of NO_x emissions in Fig. 11 refers to all sectors, as included in Vestreng et al. (2009).

449 Segregation of emissions trends by mass origin would further enlighten their possible effect on visibility variation
450 in Athens. As stated in section 2.2, air masses from the N-NE sectors dominate in Athens, contributing by more
451 than 60% on an annual basis. Following segregation of European SO₂ emissions by country as reported by
452 Mylona (1996) it comes out that emissions by countries of N-NE sector (as defined in Fig. 2a) have the largest
453 contribution in total European emissions. Sulphur dioxide emissions increased by a factor of approximately 2.5
454 between 1950 and 1980 in these regions, which is analogous to the increase of total European emissions over the
455 same period. According to Mylona (1996), the contribution of emissions from the former USSR (but also Turkey)
456 is very important after 1940. The EMEP part of USSR in particular, contributed to almost one quarter of the total
457 in the 1970s. Sulphur emissions declined after the 1990s in both eastern and western Europe, but with higher

458 rates (by a factor of 1.5) in eastern, as a result of the economic recession after 1990 in these countries (Vestreng
459 et al., 2007;Stjern et al. (2011).

460 As regards other types of emissions such as organic carbon (OC) or black carbon (BC), historical data reported
461 by Bond et al. (2007) show increase of the order of 50% on a global scale between 1930 and 2000. However,
462 segregation by region indicates that European emissions of OC and BC revealed a slight increase between 1950
463 and 1970 and decrease thereafter. Decreasing trends are also observed in the former USSR after 1970 (Bond et
464 al., 2007).

465 A very interesting finding in Fig. 11 is the similar slopes in the negative linear trends of the annual visibility at the
466 background and urban stations over their common period of observations ($-2.2 \text{ km decade}^{-1}$ and $-2.4 \text{ km decade}^{-1}$,
467 respectively). This feature implies that the inter-decadal variability of visibility in the eastern Mediterranean is
468 significantly modulated by large scale processes that control visibility, such as long-range pollution transport.
469 Many studies have identified the eastern Mediterranean as a crossroad of aerosols of different origins, sizes and
470 chemical composition (Lelieveld et al., 2002; Hatzianastassiou et al., 2009; Kanakidou et al., 2011; Gerasopoulos
471 et al., 2011), which inevitably affect optical properties of the atmosphere.

472 After the early 1990s, the two time series diverge. Background visibility at HER partly recovers, while visibility at
473 NOA keeps declining at the same pace until 2003 (Fig. 11). Recovering of visibility is also found at other Greek
474 areas around the 1990's (Lianou et al., unpublished data) which is in line with visibility improvement in other
475 European areas, related to emissions reduction (Wang et al., 2009; Vautard et al., 2009). This last feature
476 suggests that, during this period, local emissions might have a dominant role in the determination of visibility in
477 Athens.

478 A slight recovery of visibility is observed during the decade 2004-2013 (Figs. 4, 11). This improvement could be
479 attributed to a number of reasons. The years after 2004, correspond to the post Olympic Games period in Athens.
480 A number of important transport projects were completed prior to the Olympic Games in Athens in 2004. Such
481 projects are for instance the construction of the Attika Ring Road (one of the largest in Europe), the construction
482 of Tramway and the extension of Athens Metro. These projects have contributed to the reduction in the number
483 of vehicles in the city, resulting to less traffic problems and lower air pollution levels. Another possible
484 contributing factor concerns the impact of the Greek economic recession (2008-2013) on air quality in Greece,
485 and Athens in particular. Recent studies provide some evidence on this. For instance, Vrekoussis et al. (2013)
486 found strong correlation between different economic metrics and air pollutants after 2007, suggesting that the

487 economic recession has resulted in proportionally reduced levels of air pollutants in the two biggest cities in
488 Greece. This is further supported by other recent research studies that report a significant reduction in energy
489 consumption after 2008, related to the rapid economic degradation (Santamouris et al., 2013).

490 **3.6 Visibility in Athens and AOD**

491 The relationship of visibility with AOD over Athens was also explored, using two different satellite
492 based data (AVHRR and MODIS) from 1981-2009 and 2000-2014 respectively (see Section 2.5). For the AVHRR
493 AOD at 630 nm, Fig. 12a shows a 1.7% per year decrease from 1981 to 1997 and a 2.4% decrease from 1999 to
494 2009 (1998 data were not available). It is interesting to point the AOD maxima in 1991 and 1992 that are linked
495 with the Pinatubo eruption period. The AOD time series for the MODIS instrument at 550 nm showed a
496 significant and similar to AVHRR (2.4% per year) decrease from 2000 to 2010 and a further decrease of 7.4%
497 per year for the period 2010-2014 (Fig. 12b).

498 To investigate the relationship between visibility and AOD changes, the two parameters are plotted together after
499 data binning. Visibility and AOD measurements have been used as follows: Visibility at 12:00 UT was used
500 according to the indices defined in Table 2 and plotted against average AOD from synchronous satellite
501 overpasses of AVHRR and MODIS, separately. The mean AOD and its standard deviation are presented in Fig.
502 13. The AOD values are related to the visibility data, using as the distance in km the middle point of each
503 visibility bin (range). Only summertime (June-August) MODIS and AVHRR AOD have been used, to keep
504 visibility values unaffected by other atmospheric parameters like low clouds, rain, or relative humidity. It is
505 observed that for average AOD values for Athens (0.25 using the mean June-August AOD at 550 nm from our
506 MODIS AOD dataset or 0.23 at 500 nm as reported by Gerasopoulos et al., 2011), visibility varies within the
507 range of 4 km to 10 km. Under cleaner conditions (W-NW-N, 0.12-0.17 at 500 nm, Gerasopoulos et al., 2011),
508 visibility can go as high as 20 km, while very low visibility (< 0.5 km) is generally associated with the highest
509 aerosol load, with AOD > 0.3 (e.g. in the case of dust events, long-range transport of urban/industrial pollutants
510 and stagnant conditions). It has to be noted that including both satellite datasets in the same figure provides
511 information only on the summertime AOD vs visibility relationship. Average AOD from AVHRR and MODIS
512 are not directly comparable, as they represent different time periods and different wavelengths.

513 Illustrating the relationship between AOD, which consist in a vertically integrated parameter, and visibility, a
514 horizontally integrated parameter, requires various assumptions. Using satellite based AOD and visibility
515 observations for GAA, when assuming a vertically constant extinction coefficient and a mixing layer that

516 contains all aerosol load we end up describing the theoretical relationship (Koschmieder, 1924): $Vis = k / AOD$,
517 where k is a function of the mixing layer height.

518

519 **3.7 Visibility in relation to PM₁₀**

520 An additional analysis was conducted to verify the relationship between visibility and particulate pollution from
521 surface measurements, using a short dataset of PM₁₀ in Athens as described in Section 2.5. Figure 14 presents
522 visibility variation as a function of PM₁₀ levels measured at Aristotelous (urban) and Maroussi (suburban)
523 stations. Four different classes of PM₁₀ levels were used, as shown in Fig. 14. The frequency of occurrence of
524 each class is also shown in the figure. Despite the different locations and characteristics of the two stations, the
525 observed frequencies are very similar in all classes of PM₁₀ levels, with higher frequency corresponding to the
526 class of 30-60 $\mu\text{g m}^{-3}$ at both stations. The frequency of PM₁₀ > 90 $\mu\text{g m}^{-3}$ at Aristotelous is double compared to the
527 respective frequency at Maroussi. Independent of the location, the same strong relationship is observed between
528 visibility reported at NOA and PM₁₀ levels at both stations, revealing a prominent decrease of visibility with
529 increasing PM₁₀ levels, in agreement with our conclusions. Average visibility at NOA ranges between 8 and 9 km
530 under low PM₁₀ levels (< 30 $\mu\text{g m}^{-3}$), but is reduced to less than 3 km under severe episodes of particulate
531 pollution (PM₁₀ > 90 $\mu\text{g m}^{-3}$). The correlation coefficient between daily PM₁₀ levels and daily visibility at NOA
532 was found equal to -0.38 ($p < 0.05$) and -0.36 ($p < 0.05$) for Aristotelous and Maroussi sites respectively.

533 Finally, the variation of the annual averages of PM₁₀ values in Athens (Maroussi and Aristotelous stations) from
534 2004 to 2014 and at the reference site of Finokalia (available over the 10-yr period 2005-2014) are displayed in
535 Fig. 15. A decreasing tendency of PM₁₀ levels is observed at all sites, indicating changes on both local and
536 regional scale. Decreasing trends are more pronounced in Athens and particularly at Maroussi station (-2.4 $\mu\text{g m}^{-3}$
537 yr^{-1}). The decreasing trend of PM₁₀ levels is consistent with the slight improvement of visibility in Athens over the
538 same period.

539

540 **4 Discussion and Conclusions**

541 The present work analyses, for the first time, the historical record of visibility at NOA (Athens) from 1931 to
542 2013 and interprets its temporal variability and trends in terms of relevant changes in atmospheric properties
543 (related to local or regional processes) and/or meteorological conditions. Since this is the longest record of

544 visibility observations in Greece and one of the oldest in the broader area of the eastern Mediterranean, the study
545 provides unique information on the atmospheric properties of the area in the past, when air pollution records are
546 missing. The study period was divided into sub-periods corresponding to different trends in the time series of
547 visibility, each sub-period being affected by different factors.

548 The impact of meteorological conditions on visibility was investigated in different ways. Visibility in Athens was
549 found to follow a seasonal cycle, with higher visibility corresponding to the warm and dry months of the year.
550 Seasonality is more distinct in the first sub-period of the time series (1931-1948), while after the 1950s, the
551 seasonal cycle attenuates. Visibility was found to be negatively correlated with RH, the correlation being stronger
552 in the early part of the time series and attenuating over the years. On the contrary, a positive correlation between
553 visibility and wind speed was found, statistically significant during the late part of the time series, suggesting the
554 increasing role of winds on the cleanup of the atmosphere from air pollutants. Visibility was also found to be
555 sensitive to wind direction, reflecting the influence of air masses origin on visibility. Lower visibility levels are
556 constantly observed under southerly winds, corresponding to sea breeze circulation, but also to dust outbreaks.

557 The study demonstrated that visibility in Athens has undergone a prominent impairment since the early 1930s.
558 The overall trend of the annual visibility averages was found equal to $-2.8 \text{ km decade}^{-1}$. The impressively higher
559 levels of visibility in Athens before the 1950s (also characterized by strong seasonality) reflect the transparency
560 of the atmosphere at that period, coherent with the poorer aerosol load from anthropogenic emissions (urban
561 and/or regional). The dramatic decrease of the visual air quality in the 1950s coincides with a number of events
562 (end of wars, rapid urbanization and rapid increase of anthropogenic emissions on local and regional scale) and
563 points to the prominent role of aerosol load in the atmosphere of Athens. Air pollution has gradually incurred a
564 severe visual pollution in the city, with visibility lower than 4 km corresponding to more than half of the year
565 during the decade 2004-2013.

566 The comparison of the annual averages of visibility in Athens and at a reference, non urban site (HER) in Crete,
567 revealed similar and statistically significant negative trends at both sites, suggesting the major contribution of
568 long and regional range transport of natural and anthropogenic pollution sources in the GAA. An improvement of
569 visibility at HER around the 1990s was not associated with synchronous improvement of visibility in Athens,
570 where visibility deterioration continued until the early 2000s. Although negative trends of main gaseous air
571 pollutants are reported in Athens at that period (Kalabokas et al., 1999a), the direct effect of such pollutants on
572 light extinction is negligible compared to suspended particles and particularly to fine particles ($<1 \mu\text{m}$).

573 A strong anticorrelation was found between visibility and PM_{10} levels in Athens, measured at two different
574 stations (urban and suburban) over the period 2008-2012 (Fig. 14). The relationship between AOD and visibility
575 in Athens was also examined in the study, using MODIS and AVHRR satellite data (Figs 12, 13), and confirmed
576 their negative correlation.

577 The analysis showed a recent stabilization (or even slight improvement) of visibility in Athens, consistent with the
578 observed decreasing trends of PM_{10} in the city from 2004 to 2014 (Fig. 15). This could possibly be related to
579 reduced local anthropogenic emissions as a result of important transport infrastructures, but also of the economic
580 recession in Greece. Although this last argument is already supported by some recent research studies, the impact
581 of economic recession on local emissions seems to be more complicated and drawing conclusions remains
582 tentative. Besides, in the same period, regional atmospheric pollution presents a decreasing tendency (Fig.
583 15), which is also consistent with the recent recovery of visibility in Athens.

584 The 82-years long time series of visibility in Athens unfolded for first time information on the atmospheric
585 conditions over the area, for periods when atmospheric pollution measurements are missing. Although the
586 analysis is subject to several limitations and assumptions, associated to the methods of visibility observations, the
587 results are robust and statistically significant, as the outstanding degradation of the visual air quality in the city
588 over the years.

589

590 **Acknowledgments.** The study is a contribution to the ChArMEX (The Chemistry-Aerosol Mediterranean
591 Experiment) work package on variability and trends. The study was supported by the Excellence Research
592 Program GSRT- Siemens (2015-2017) ARISTOTELIS "Environment, Space and Geodynamics/Seismology
593 2015-2017" in the framework of the Hellenic Republic-Siemens settlement Agreement. The authors are grateful
594 to the Editor Dr. François Dulac and the two anonymous reviewers, for their very useful comments and
595 suggestions on this study. The authors would also like to thank the Hellenic National Meteorological Service
596 (HNMS) for the provision of visibility data at Heraklion (Crete) and the Air Quality Department of the Ministry
597 of Environment & Energy of Greece for the provision of air pollution data. The contribution of Mr. F. Pierros
598 (NOA) and Mrs D. Koutentaki (NOA) in the digitization of visibility data of NOA and of Dr. G. Kouvarakis
599 (University of Crete) in the analysis of air trajectories is also acknowledged.

600

601 **References**

- 602 Appel, B.R., Tokiwa, Y., Hsu, J., Kothny, E., and Hahn, E.: Visibility as related to atmospheric aerosol
603 constituents, *Atmos. Environ.*, 19, 1525-1534, doi:10.1016/0004-6981(85)90290-2, 1985.
- 604 Bäumer, D., Vogel, B., Versick, S., Rinke, R., Möhler, O., and Schnaiter, M.: Relationship of visibility, aerosol
605 optical thickness and aerosol size distribution in an ageing air mass over South-West Germany, *Atmos. Environ.*,
606 42, 989-998, doi:10.1016/j.atmosenv.2007.10.017, 2008.
- 607 Bond, T.C., Bhardwaj, E., Dong, R., Jogani, R., Jung, S., Roden, C., Streets, D.G., and Trautmann, N.M.:
608 Historical emissions of black and organic carbon aerosol from energy-related combustion, 1850-2000, *Glob.*
609 *Biochem. Cycles*, 21, GB2018, doi:10.1029/2006GB002840, 2007.
- 610 Carapiperis, L.N., and Karapiperis, P.P.: On the ocean colour of the sky in Athens, *Academy of Athens*, 27, 213,
611 1952.
- 612 Cermak, J., Wild, M., Knutti, R., Mishchenko M.I., and Heidinger, A.K.: Consistency of global satellite-derived
613 aerosol and cloud data sets with recent brightening observations, *Geophys. Res. Lett.*, 37, L21704,
614 doi:10.1029/2010GL044632, 2010.
- 615 Chaloulakou, A., Kassomenos, P., Spyrellis, N., Demokritou, P., and Koutrakis, P.: Measurements of PM₁₀ and
616 PM_{2.5} particle concentrations in Athens, Greece, *Atmos. Environ.*, 37, 649 – 660, doi:10.1016/S1352-
617 2310(02)00898-1, 2003.
- 618 Chan, Y.C., Simpson, R.W., Mctainsh, G.H., Vowles, P.D., Cohen, D.D., and Bailey, G.M.: Source
619 apportionment of visibility degradation problems in Brisbane (Australia) using the multiple linear regression
620 techniques, *Atmos. Environ.*, 33, 3237–3250, doi:10.1016/S1352-2310(99)00091-6, 1999.
- 621 Chan, P.K., Zhao, X.P., and Heidinger, A.K.: Long-Term Aerosol Climate Data Record Derived from Operational
622 AVHRR Satellite Observations, *Dataset Papers in Geosciences*, vol. 2013, Article ID 140791, 5 pages, 2013.
623 doi:10.7167/2013/140791, 2013.
- 624 Chang, D., Song, Y., and Liu, B.: Visibility trends in six megacities in China 1973–2007, *Atmos. Res.*, 94, 161–
625 167, doi:10.1016/j.atmosres.2009.05.006, 2009.
- 626 Che, H.Z., Zhang, X.Y., Li, Y., Zou, Z.J., and Qu, J.J.: Horizontal visibility trends in China 1981-2005, *Geophys.*
627 *Res. Lett.*, 34, L24706, doi:10.1029/2007GL031450, 2007.
- 628 Colbeck, I., Chung, M.C., and Eleftheriadis, K.: Formation and transport of atmospheric aerosol over Athens,
629 Greece, *Water Air Soil Pollut.*, 223-235, doi:10.1023/A:1021335401558, 2002.
- 630 Davis, R.E.: A synoptic climatological analysis of winter visibility trends in the mideastern United States, *Atmos.*
631 *Environ.*, 25b, 165-175, doi:10.1016/0957-1272(91)90052-G, 1991.

- 632 Dayan, U., and Levy, I.: The Influence of Meteorological Conditions and Atmospheric Circulation Types on
633 PM10 and Visibility in Tel Aviv, *J. Appl. Meteorol.*, 44, 606-619, doi: /10.1175/JAM2232.1, 2005.
- 634 Deng, J.J., Wang, T.J., Jiang, Z.Q., Xie, M., Zhang, R.J., Huang, X.X., and Zhu, J.L.: Characterization of
635 visibility and its affecting factors over Nanjing, China, *Atmos. Res.*, 101, 681-691,
636 doi:10.1016/j.atmosres.2011.04.016, 2011.
- 637 Doyle, M., and Dorling, S.: Visibility trends in the UK 1950-1997, *Atmos. Environ.*, 36, 3161-3172,
638 doi:10.1016/S1352-2310(02)00248-0, 2002.
- 639 Draxler, R., Stunder, B., Rolph, G., Stein, A., and Taylor, A.: Hybrid Single-Particle Lagrangian Integrated
640 Trajectories (HY-SPLIT): Version 4.9 - User's Guide and Model Description,
641 [http://www.arl.noaa.gov/documents/reports/hysplit user guide.pdf](http://www.arl.noaa.gov/documents/reports/hysplit%20user%20guide.pdf),2009.
- 642 Eidels-Dubovoi, S.: Aerosol impacts on visible light extinction in the atmosphere of Mexico City, *Sci. Total*
643 *Environ.*,287, 213-220, doi:10.1016/S0048-9697(01)00983-4, 2002.
- 644 Elias, T., Haeffelin, M., Drobinski, P., Gomes, L., Rangognio, J., Bergot, T., Chazette, P., Raut, J.C., and
645 Colomb, M.: Particulate contribution to extinction of visible radiation: pollution, haze, and fog, *Atmos. Res.*, 92,
646 443-454, doi:10.1016/j.atmosres.2009.01.006, 2009.
- 647 Eltbaakh Y.A., Ruslan, M.H., Alghoul, M.A., Othman, M.Y., and Sopian, K.: Issues concerning atmospheric
648 turbidity indices, *Renw. Sustain. Energy Rev.*, 16, 6285-6294, doi: 10.1016/j.rser.2012.05.034, 2012.
- 649 Folini, D., and Wild, M.: Aerosol emissions and dimming/brightening in Europe: Sensitivity studies with
650 ECHAM5-HAM, *J. Geophys. Res.*, 116, D21, doi:10.1029/2011JD016227, 2011.
- 651 Founda, D.: Evolution of the air temperature in Athens and evidence of climatic change: A review, *Advances in*
652 *Building Energy Research*, 5, 7- 41, doi:10.1080/17512549.2011.582338, 2011.
- 653 Founda, D.,Pierros, F., Petrakis, M., and Zerefos, C.: Inter-decadal variations and trends of the Urban Heat Island
654 in Athens (Greece) and its response to heat waves,*Atmos. Res.*,161, 1-13. doi:10.1016/j.atmosres.2015.03.016,
655 2015.
- 656 Gerasopoulos, E., Kouvarakis, G., Vrekoussis, M., Kanakidou, M., and Mihalopoulos, N.: Ozone variability in
657 the marine boundary layer of the Eastern Mediterranean based on 7-year observations, *J. Geophys. Res.*, 110,
658 D15309, doi:10.1029/2005JD005991, 2005.
- 659 Gerasopoulos, E., Amiridis, V., Kazadzis, S., Kokkalis, P., Eleftheratos, K., Andreae, M.O., Andreae, T.W., El-
660 Askary, H., and Zerefos, C.S.: Three-year ground based measurements of aerosol optical depth over the Eastern

- 661 Mediterranean: The urban environment of Athens, *Atmos. Chem. Phys.*, 11, 2145-2159, doi:10.5194/acp-11-
662 2145-2011, 2011.
- 663 Ghim, Y.S., Moon, K., Lee, S., and Kim, Y.P.: Visibility trends in Korea during the past two decades, *J. Air*
664 *Waste Manage Assoc.*, 55, 73-82, doi:10.1080/10473289.2005.10464599, 2005.
- 665 Gkikas, A., Basart, S., Hatzianastassiou, N., Marinou, E., Amiridis, V., Kazadzis, S., Pey, J., Querol, X., Jorba,
666 O., Gassó, S., and Baldasano, J. M.: Mediterranean desert dust outbreaks and their vertical structure based on
667 remote sensing data, *Atmos. Chem. Phys.*, 15, 27675-27748, doi:10.5194/acpd-15-27675-2015, 2015.
- 668 Grivas, G., Chaloulakou, A., Samara, C., and Spyrellis, N.: Spatial and temporal variation of PM10 mass
669 concentrations within the Greater Area of Athens, Greece, *Water Air Soil Pollut.*, 158, 357-71,
670 doi:10.1023/B:WATE.0000044859.84066.09, 2004.
- 671 Hamonou, E., Chazette, P., Balis, D., Dulac, F., Schneider, X., Galani, E., Ancellet, G., and Papayannis, A.:
672 Characterization of the vertical structure of Saharan dust export to the Mediterranean basin, *J. Geophys. Res.*, 104,
673 22257-22270, doi:10.1029/1999JD900257, 1999.
- 674 Hand, J.L., Kreidenweis, S.M., Sherman, D.E., Collett, Jr J.L., Hering, S.V., Day, D.E, and Malm, W.C.: Aerosol
675 size distributions and visibility estimates during the Big Bend Regional Aerosol and Visibility Observational
676 (BRAVO) study, *Atmos. Environ.*, 36, 5043-5055, doi:10.1016/S1352-2310(02)00568-X, 2002.
- 677 Hatzianastassiou, N., Gkikas, A., Mihalopoulos, N., Torres, O., and Katsoulis, B.D.: Natural versus
678 anthropogenic aerosols in the eastern Mediterranean basin derived from multiyear TOMS and MODIS satellite
679 data, *J. Geophys. Res.*, 114, D24202, doi:10.1029/2009JD011982, 2009.
- 680 Hoek, G., Forsberg, B., Borowska, M., Hlawiczka, S., Vaskovi, E, Welinder, H., et al.: Wintertime PM10 and
681 black smoke concentrations across Europe: results from the Peace study, *Atmos. Environ.*, 31, 3609-3622,
682 doi:10.1016/S1352-2310(97)00158-1, 1997.
- 683 Ichoku, C., Chu, D.A., Mattoo, S. et al.: A spatio-temporal approach for global validation and analysis of MODIS
684 aerosol products, *Geophys. Res. Lett.*, 29, 1- 4, doi:10.1029/2001GL013206, 2002.
- 685 Kalabokas, P.D., Viras, L.G., and Repapis, C.C.: Analysis of 11-year record (1987-1997) of air pollution
686 measurements in Athens, Greece, Part I: primary air pollutants, *Global Nest*, 1, 157-167, 1999a.
- 687 Kalabokas, P.D., Viras, L.G., Repapis, C.C., and Bartzis, J.G.: Analysis of 11-year record (1987-1997) of air
688 pollution measurements in Athens, Greece, Part II: photochemical air pollutants, *Global Nest*, 1, 169-176, 1999b.
- 689 Kanakidou, M., Mihalopoulos, N., Kindap, T., Im, U. et al.: Megacities as hot spots of air pollution in the East
690 Mediterranean, *Atmos. Environ.*, 45, 1223-1235, doi:10.1016/j.atmosenv.2010.11.048, 2011.

- 691 Kanellopoulou, E.: Study of the visibility of Athens. PhD Thesis (in Greek), 1979.
- 692 Kim, K.W.: Physico-chemical characteristics of visibility impairment by airborne pollen in an urban area,
693 *Atmos. Environ.*, 41, 3565–357, doi:10.1016/j.atmosenv.2006.12.054, 2007.
- 694 Kim, K.W.: Optical Properties of Size-Resolved Aerosol Chemistry and visibility Variation Observed in the
695 Urban Site of Seoul, Korea, *Aerosol Air Qual. Res.*, 15, 271–283, doi: 10.4209/aaqr.2013.11.0347, 2015.
- 696 Koschmieder, H.: Theorie der horizontalen sichtweite, *Beitr. Phys. Frei. Atmos.*, 12, 171–181, 1924.
- 697 Kouvarakis G., Tsigaridis, K., Kanakidou, M., and Mihalopoulos, N.: Temporal variations of surface regional
698 background ozone over Crete Island in southeast Mediterranean, *J. Geophys. Res.*, 105, 4399-4407,
699 doi:10.1029/1999JD900984,2000.
- 700 Larson, S.M., and Cass, G.R.: Characteristics of summer midday low-visibility events in the Los Angeles area,
701 *Environ. Sci. Technol.*, 23, 281–289, doi: 10.1021/es00180a003,1989.
- 702 Lee, D.O.: Regional variations in long-term visibility trends in the UK (1962–1990), *Geog.*, 79, 108–121,
703 <http://www.jstor.org/stable/40572408>, 1994.
- 704 Léon, J.-F., Chazette, P., and Dulac, F.: Retrieval and monitoring of aerosol optical thickness over an urban area
705 by spaceborne and ground-based remote sensing, *Appl. Opt.*, 38, 6918-6926, doi:10.1364/AO.38.006918, 1999
- 706 Lelieveld, J., Berresheim, H., Borrmann, S., Crutzen, P.J., et al.: Global Air Pollution Crossroads over the
707 Mediterranean, *Science*,298,794-799, doi: 10.1126/science.1075457, 2002.
- 708 Malm, W.C.: Introduction to Visibility, Air Resources Division, National Park Service, Cooperative Institute for
709 Research in the Atmosphere (CIRA), NPS Visibility Program, Colorado State University, Fort Collins, CO, May,
710 1999.
- 711 Maloutas, T.: The self promoting housing solution in post war Athens, Discussion Paper Series 9(6) 95-110,
712 Available online at: http://www.prd.uth.gr/research/DP/2003/uth-prd-dp-2003-6_en.pdf, 2003.
- 713 Mavroidis, I., and Iliá, M.: Trends of NO_x,NO₂ and O₃ concentrations, at three different types of air quality
714 monitoring stations in Athens, Greece, *Atmos. Environ.*, 63,135–147, doi:10.1016/j.atmosenv.2012.09.030, 2012.
- 715 Mishchenko, M.I., Geogdzhayev, I.V., Rossow, W.B., Cairns, B., Carlson, B.E., Laciš, A.A., Liu, L., and Travis,
716 L.D.: Long-term satellite record reveals likely recent aerosol trend, *Science*, 315, no. 5818, p. 1543,
717 doi:10.1126/science.1136709, 2007.

- 718 Mylona, S.: Sulfur dioxide emissions in Europe 1880-1991 and their effect on sulphur concentrations and
719 depositions, *Tellus*, 48, 662-689, doi/10.1034/j.1600-0889.1996.t01-2-00005.x, 1996.
- 720 Nabat, P., Somot, S., Mallet, M., Sanchez-Lorenzo, A., and Wild, M.: Contribution of anthropogenic sulfate
721 aerosols to the changing Euro-Mediterranean climate since 1980, *Geophys. Res. Lett.*, 41, 5605-5611,
722 doi:10.1002/2014GL060798, 2014.
- 723 Paraskevopoulou, D., Liakakou, E., Gerasopoulos, E., Theodosi, C., and Mihalopoulos, N.: Long-term
724 characterization of organic and elemental carbon in the PM_{2.5} fraction: the case of Athens, Greece, *Atmos. Chem.*
725 *Phys.*, 14, 13313–13325, doi:10.5194/acp-14-13313-2014, 2014.
- 726 Paraskevopoulou, D., Liakakou, E., Gerasopoulos, E., and Mihalopoulos, N.: Sources of atmospheric aerosols
727 from long-term measurements (5 years) of chemical composition in Athens, Greece, *Sci. Total Environ.*, 527–
728 528, 165–178, doi:10.1016/j.scitotenv.2015.04.022, 2015.
- 729 Remoudaki, E., Gergametti, G., and Losno, R.: On the dynamic of the atmospheric input of copper and
730 manganese into the western Mediterranean Sea, *Atmos. Environ.*, 25A, 733-744, doi:10.1016/0960-
731 1686(91)90072-F, 1991a.
- 732 Remoudaki, E., Gergametti, G., and Buat-Ménard, P.: Temporal variability of atmospheric lead concentrations
733 and fluxes over the northwestern Mediterranean Sea, *J. Geophys. Res.*, 96, 1043-1055, doi:10.1029/90JD00111,
734 1991b.
- 735 Santamouris, M., Paravantis, J.A., Founda, D., Kolokotsa, D., Michalakakou, P., Papadopoulos, A.M.,
736 Kontoulis, N., Tzavali, A., Stigka, E.K., Ioannidis, Z., Mehilli, A., Matthiessen, A., and Servou, E.: Financial
737 Crisis and Energy Consumption: A household Survey in Greece, *Energy Build.*, 65, 477-487,
738 doi:10.1016/j.enbuild.2013.06.024, 2013.
- 739 Singh, A., and Dey, S.: Influence of aerosol composition on visibility in megacity Delhi, *Atmos. Environ.*, 62,
740 367- 373,doi:10.1016/j.atmosenv.2012.08.048, 2012.
- 741 Sloane, C.S.: Visibility trends - II. Mideastern United States 1948-1978, *Atmos. Environ.*, 16, 2309-2321,
742 doi:10.1016/0004-6981(82)90117-2, 1982.
- 743 Smirnov, A., Holben, B. N., Sakerin, S.M., Kabanov, D. M., Slutsker, I., Chin, M., Diehl, T.L., Remer, L.A.,
744 Kahn, R.A., Ignatov, A., Liu, L., Mishchenko, M., Eck, T.F., Kucsera, T.L., Giles, D.M., and Kopelevich, O.V.:
745 Ship-based aerosol optical depth measurements in the Atlantic Ocean, comparison with satellite retrievals and
746 GOCART model, *Geophys. Res. Lett.*, 33, L14817, doi:10.1029/2006GL026051, 2006.

- 747 Stjern, C.W., Stohl, A., and Kristjánsson, J.E.: Have aerosols affected trends in visibility and precipitation in
748 Europe? *J. Geophys. Res.*, 116, D02212, doi:10.1029/2010JD014603, 2011.
- 749 Streets, D.G., Wu, Y., and Chin, M.: Two-decadal aerosol trends as a likely explanation of the
750 global dimming/brightening transition, *Geophys. Res. Lett.*, 33, L15806, doi:10.1029/2006GL026471, 2006.
- 751 Tang, I.N.: Chemical and size effects of hygroscopic aerosols on light scattering coefficients, *J. Geophys. Res.*,
752 101, 19245–19250, doi: 10.1029/96JD03003, 1996.
- 753 Theodosi, C., Grivas, G., Zampas, P., Chaloulakou, A., and Mihalopoulos, N.: Mass and chemical composition
754 of size-segregated aerosols (PM₁, PM_{2.5}, PM₁₀) over Athens, Greece: local versus regional sources, *Atmos.*
755 *Chem. Phys.*, 11, 11895–11911, doi:10.5194/acp-11-11895-2011, 2011.
- 756 Tsai, Y.I., Lin, Y.H., and Lee, S.Z.: Visibility variation with air qualities in the metropolitan area of southern
757 Taiwan, *Water Air Soil Pollut.*, 144, 19-40, doi:10.1023/A:1022901808656, 2003.
- 758 Tsai, Y.I., Kuo, S.C., Lee, W.J., Chen, C.L., and Chen, P.T.: Long-term visibility trends in one highly urbanized,
759 one highly industrialized, and two rural areas of Taiwan, *Sci. Total Environ.*, 382, 324–341,
760 doi:10.1016/j.scitotenv.2007.04.048, 2007.
- 761 van Aardenne, J.A., Dentener, F.J., Olivier, J.G.J., Klein Goldewijk, C.G. M., and Lelieveld, J.: A 1°×1°
762 resolution data set of historical anthropogenic trace gas emissions for the period 1890–1990, *Glob. Biochem.*
763 *Cycles*, 15, 909-928, doi: 10.1029/2000GB001265, 2001.
- 764 van Beelen, A.J., and van Delden, A.J.: Cleaner air brings better views, more sunshine and warmer summer days
765 in the Netherlands, *Weather*, 67, 21-25, doi: 10.1002/wea.854, 2012.
- 766 Vautard, R., Yiou, P., and Oldenborgh, G.: Decline of fog, mist and haze in Europe over the past 30 years, *Nat.*
767 *Geosci.*, 2, 115-119, doi:10.1038/NGEO414, doi:10.1038/ngeo414, 2009.
- 768 Vestreng, V., Ntziachristos, L., Semb, A., Reis, S., Isaksen, I.S.A., and Tarrasón, L.: Evolution of NO_x emissions
769 in Europe with focus on road transport control measures, *Atmos. Chem. Phys.*, 9, 1503-1520, doi: 10.5194/acp-9-
770 1503-2009, 2009.
- 771 Vestreng, V., Myhre, G., Fagerli, H., Reis, S., and Tarrasón, L.: Twenty five years of continuous sulphur dioxide
772 emission reduction in Europe, *Atmos. Chem. Phys.*, 7, 3663-3681, doi:10.5194/acp-7-3663-2007, 2007.
- 773 Vrekoussis, M., Richter, A., Hilboll, A., Burrows, J.P., Gerasopoulos, E., Lelieveld, J., Barrie, L., Zerefos, C.,
774 and Mihalopoulos, N.: Economic crisis detected from space: Air quality observations over Athens, Greece,
775 *Geophys. Res. Lett.*, 40, 458-463, doi:10.1002/grl.50118, 2013.

776 Wan, J.M., Lin, M., Chan, C.Y., Zhang, Z.S., Engling, G., Wang, X.M., Chan, I.N., and Li, S.Y.: Change of air
777 quality and its impact on atmospheric visibility in central-western Pearl River Delta, *Environ. Monit. Assess.*,
778 172, 339-351, doi: 10.1007/s10661-010-1338-2, 2011.

779 Wang, K., Dickinson, R.E., and Liang, S.: Clear sky visibility has decreased over land globally from 1973 to
780 2007, *Science*, 323, 1468-1470, doi:10.1126/science.1167549, 2009.

781 Wang, K.C., Dickinson, R.E., Su, L., and Trenberth, K.E.: Contrasting trends of mass and optical properties of
782 aerosols over the Northern Hemisphere from 1992 to 2011, *Atmos. Chem. Phys.*, 12, 9387–9398,
783 doi:10.5194/acp-12-9387-2012, 2012.

784 Wild, M., 2009: Global dimming and brightening: A review, *J. Geophys. Res.*, 114, doi: 10.1029/2008JD011470,
785 2009.

786 Wu, J., Fu, C., Zhang, L., and Tang, J.: Trends of visibility on sunny days in China in the recent 50 years, *Atmos.*
787 *Environ.*, 5, 339-346, doi:10.1016/j.atmosenv.2012.03.037, 2012.

788 World Meteorological Organization: The WMO Automatic Digital Barometer inter comparison (J. P. van der
789 Meulen), Instrument and Observing Methods Report No.46, WMO/TD-No.474, Geneva, 1992.

790 Zhao, P., Zhang, X., Xu, X. and Zhao, X.: Long-Term Visibility Trends and Characteristics in the Region of
791 Beijing, Tianjin, and Hebei, China, *Atmos. Res.*, 101, 711–718, doi:10.1016/j.atmosres.2011.04.019, 2011.

792 Zhao X., Chan, P., and NOAA CDR Program: NOAA Climate Data Record (CDR) of AVHRR Daily and
793 Monthly Aerosol Optical Thickness over Global Oceans, Version 2.0. AOT1, NOAA National Centers for
794 Environmental Information. doi:10.7289/V5SB43PD, 2014.

795

796

797

798 Table 1: Mean monthly and yearly values with standard deviations of basic climatic elements in Athens (NOA),
 799 calculated from the WMO climatic period (1971-2000). (**)

Month	Tmean (°C)	Tmax (°C)	Tmin (°C)	RH (%)	Rainfall (mm)	Number of rainy days (> 1mm)	Wind Speed (m s ⁻¹)
January	9.3 ±1.1	13.0 ±1.3	6.6 ±1.1	72.1 ±3.9	42.5 ±31	5.6 ± 3.0	3.1 ± 0.71
February	9.6 ±1.4	13.7 ±1.7	6.8 ±1.4	70.2 ±3.5	44.8 ±29	5.6 ± 2.1	3.4 ± 0.50
March	11.5 ± 1.4	16.1 ± 1.8	8.2 ± 1.3	67.6 ± 4.3	50.2 ± 41	5.4 ± 2.6	3.3 ± 0.72
April	15.4 ± 1.3	20.5 ± 1.6	11.5 ± 1.1	62.7 ± 4.6	32.7 ± 29	4.2 ± 2.6	2.8 ± 0.51
May	20.3 ± 1.1	25.7 ± 1.3	16.1 ± 1.1	57.3 ± 4.0	16.7 ± 16	2.6 ± 1.9	2.9 ± 0.45
June	25.0 ± 0.9	30.6 ± 1.2	20.4 ± 0.9	51.3 ± 3.7	7.5 ± 10	0.9 ± 1.0	3.1 ± 0.60
July	27.3 ± 1.1	33.1 ± 1.4	22.7 ± 1.1	48.5 ± 4.2	6.6 ± 9	0.9 ± 1.1	3.5 ± 0.75
August	26.8 ± 1.2	33.7 ± 1.4	22.5 ± 1.2	49.8 ± 5.1	7.2 ± 12	0.9 ± 1.2	3.5 ± 0.58
September	23.4 ± 1.1	29.2 ± 1.5	19.4 ± 1.0	57.0 ± 4.7	9.4 ± 1	1.3 ± 1.6	2.9 ± 0.47
October	18.5 ± 1.5	23.5 ± 1.8	15.1 ± 1.6	66.4 ± 3.7	42.9 ± 40	3.7 ± 2.4	2.9 ± 0.74
November	14.0 ± 1.3	18.1 ± 1.5	11.1 ± 1.3	72.7 ± 3.8	59.9 ± 45	7.9 ± 3.8	2.9 ± 0.73
December	10.8 ± 1.4	14.4 ± 1.8	8.2 ± 1.3	74.0 ± 3.2	62.6 ± 34	9.0 ± 13.4	3.0 ± 0.56
Year	17.7 ± 0.5	22.6 ± 0.7	14.1 ± 0.5	62.0 ± 1.9	389.5 ± 5	42.9 ± 9.0	3.1 ± 0.36

800 (***) Climatic means were calculated from daily observations at NOA over the period 1971-2000. Daily time series are
 801 almost complete, with sporadic missing data in certain variables. In particular, data availability for the period 1971-2000 is
 802 100% for Tmax, Tmin and rainfall, 99.9 % for Tmean, 99.8 % for RH and 99.4% for the wind speed.
 803
 804

805

806 Table 2: The WMO empirical scale for visibility observations,used at NOA.

Visibility Classes	1	2	3	4	5	6	7	8	9
Visibility Ranges	50- 200m	200- 500m	500- 1000m	1-2 km	2-4 km	4-10 km	10-20 km	20-50 km	>50km

807

808

809

810

811

812

813

814

815

816

817

818

819

820

821

822

823

824
825
826
827
828
829
830
831
832
833
834
835
836
837
838
839
840
841
842
843
844
845

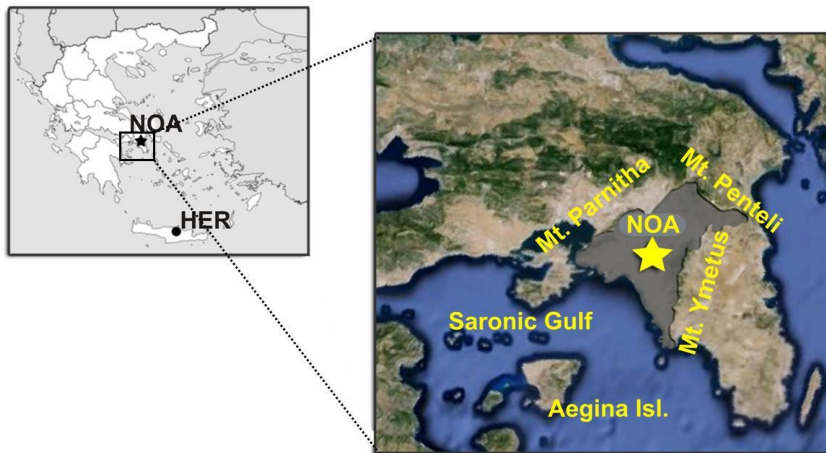


Fig.1. Map of the study area in Greece, including the Athens urban station (NOA) and the reference, non-urban station (HER) at Heraklion airport, Crete. The grey surface represents the boundary of the Greater Athens Area (GAA).

846

847

848

849

850

851

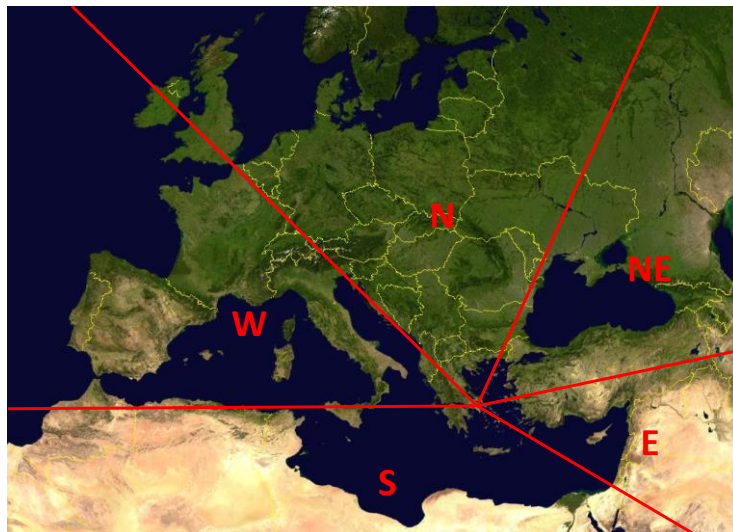
852

853

854

855

856



857

Fig. 2a. Main sectors related to air masses origin in Athens.

858

859

860

861

862

863

864

865

866

867

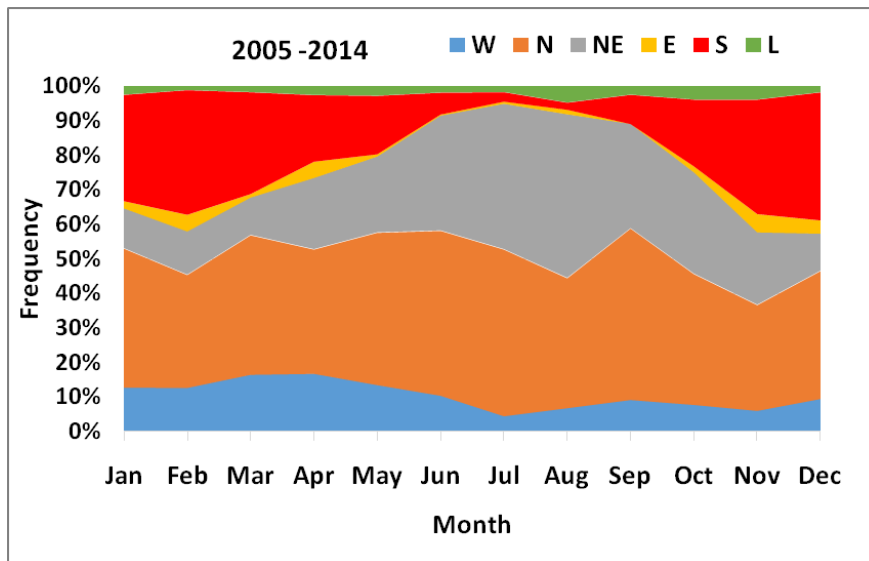


Fig.2b. Seasonal variability of the relative frequency of air masses origin in Athens on the sectors defined in Fig. 2a, averaged over the period 2005-2014. Category 'L' refers to air masses of local origin.

890
 891
 892
 893
 894
 895
 896
 897
 898
 899
 900
 901
 902
 903
 904
 905
 906
 907
 908
 909
 910

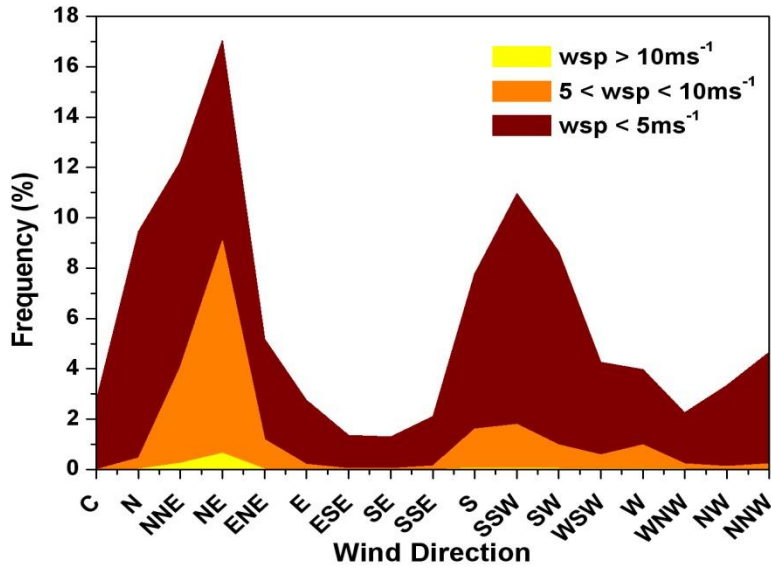
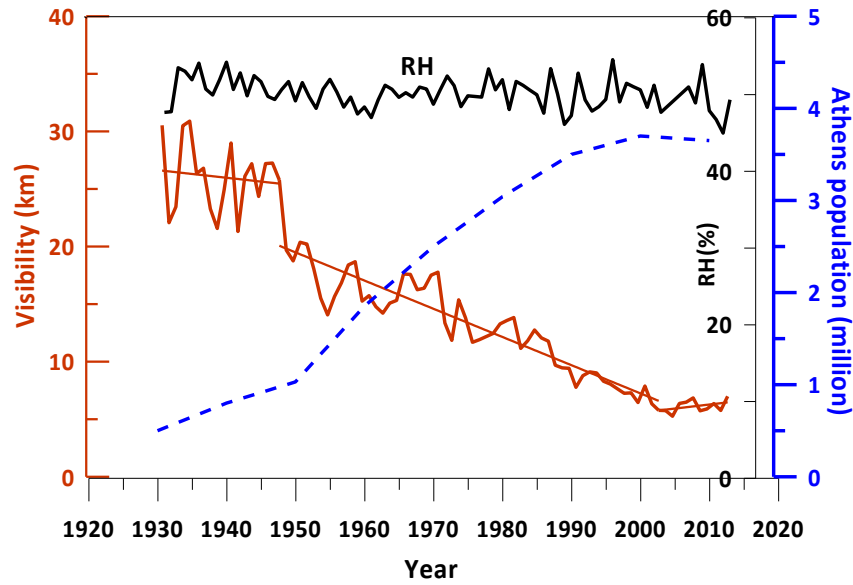


Fig.3. Frequencies of surface wind directions for three wind speed (wsp) categories at NOAA, based on hourly values of the period 1971-2000. For instance, the NE direction occurs cumulatively at a frequency of 17% which is the sum of 7.9% ($wsp < 5\text{ms}^{-1}$), 8.4% ($5 < wsp < 10\text{ms}^{-1}$) and 0.7% ($wsp > 10\text{ms}^{-1}$). The 'C' sector corresponds to calms ($wsp < 0.3\text{ms}^{-1}$).

911
912
913



914

915 **Fig. 4.** Inter-decadal variability of the annual visibility in Athens from 1931 to 2013, along with linear trends for
916 three sub-periods: 1931-1948, 1949-2003 and 2004-2013 (red line). The dashed blue line illustrates the
917 population growth in Athens (in millions) since 1930 (Founda, 2011). The long-term variability of the annual
918 relative humidity (RH) in Athens is also shown (upper black line).

919

920

921

922

923

924

925

926

927
928
929
930
931
932
933
934
935
936
937
938
939
940
941
942
943
944
945
946
947

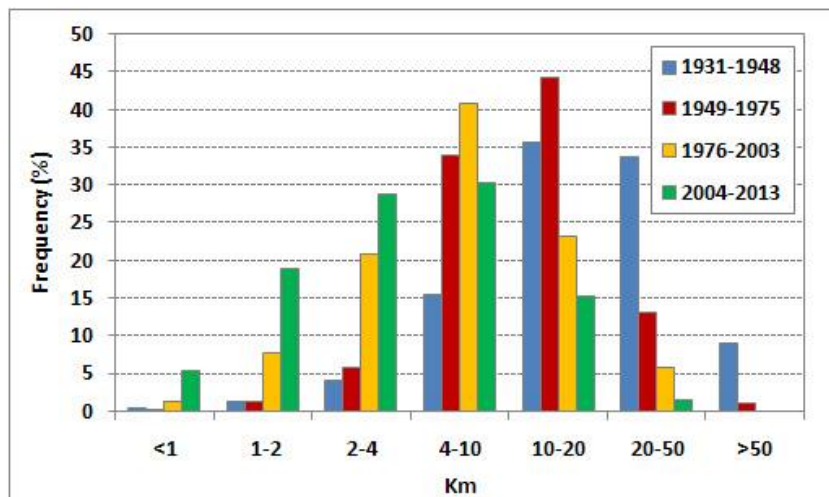
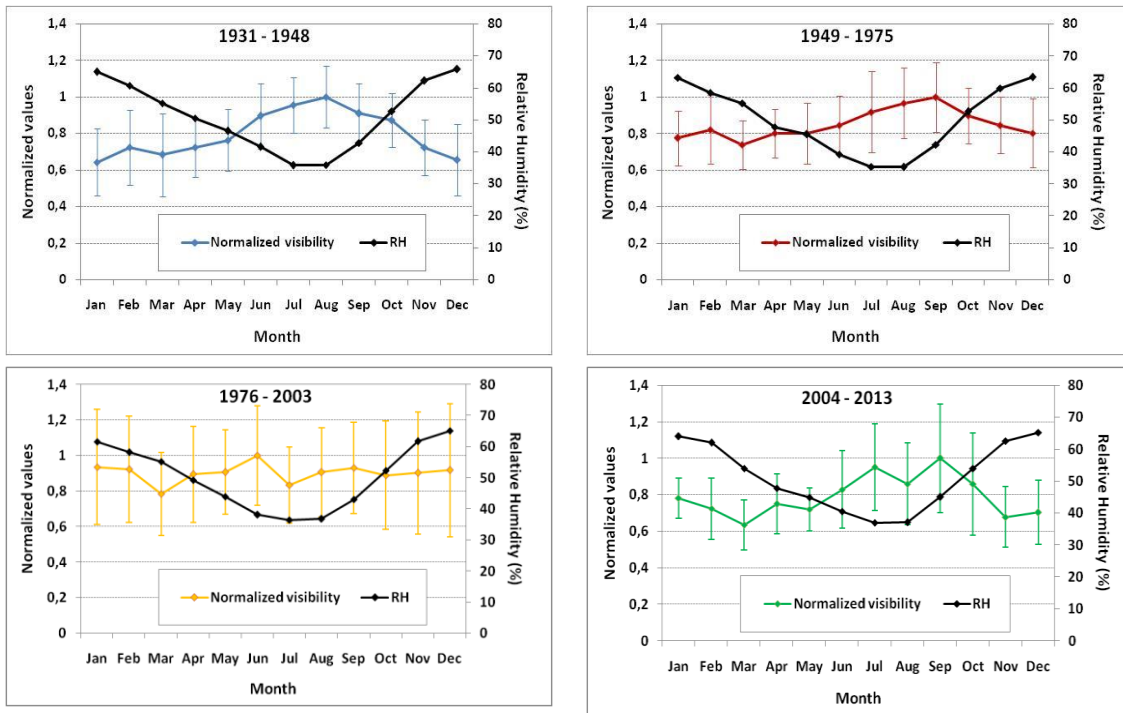


Fig. 5. Frequency distribution of different visibility ranges (as defined in Table 2) in Athens for the sub-periods 1931-1948, 1949-1975, 1976-2003 and 2004-2013.

948
949
950



951

952 **Fig. 6.** Normalized mean monthly values of visibility in Athens for the sub-periods 1931-1948, 1949-1975, 1976-
953 2003 and 2004-2013, along with mean monthly values of relative humidity (RH) for each sub-period. Vertical
954 lines represent standard deviations of mean monthly values of visibility.

955

956

957

958

959

960
961
962
963
964
965
966
967
968
969
970
971
972
973
974
975
976
977
978
979
980
981
982

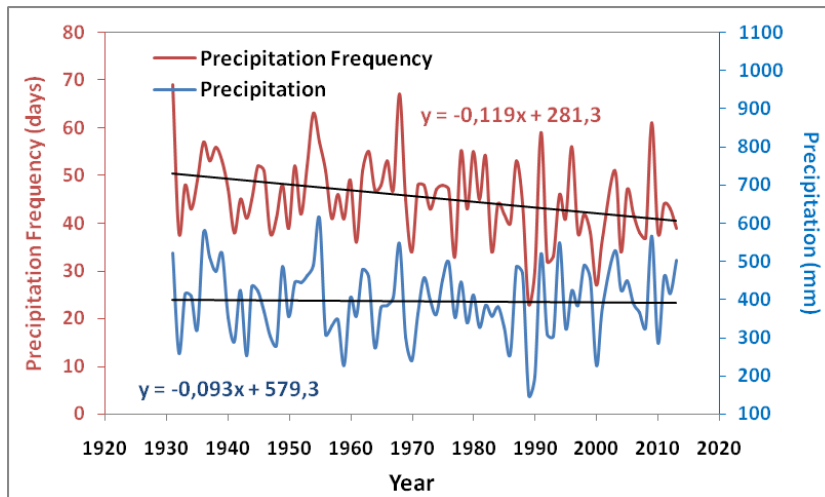


Fig. 7. Long-term variability and linear trends of the annual precipitation amount and precipitation frequency (number of days/year,with precipitation > 1mm) at NOAA, over the period 1931-2013. Slopes of linear trends are also shown.

983
984
985
986
987
988
989
990
991
992
993
994
995
996
997
998
999
1000
1001
1002
1003
1004
1005
1006

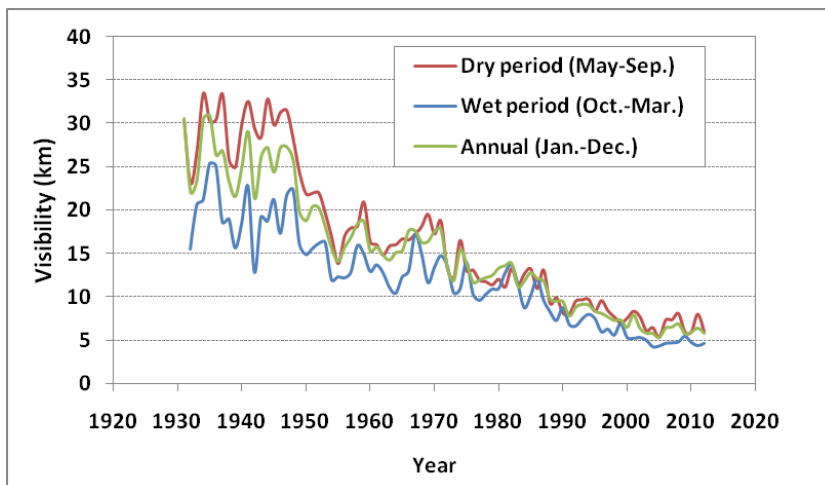


Fig.8. Variation of visibility at NOA from 1931-2013 during the dry (May-Sep.), wet (Oct.-Mar.) and all year (Jan.-Dec.) period.

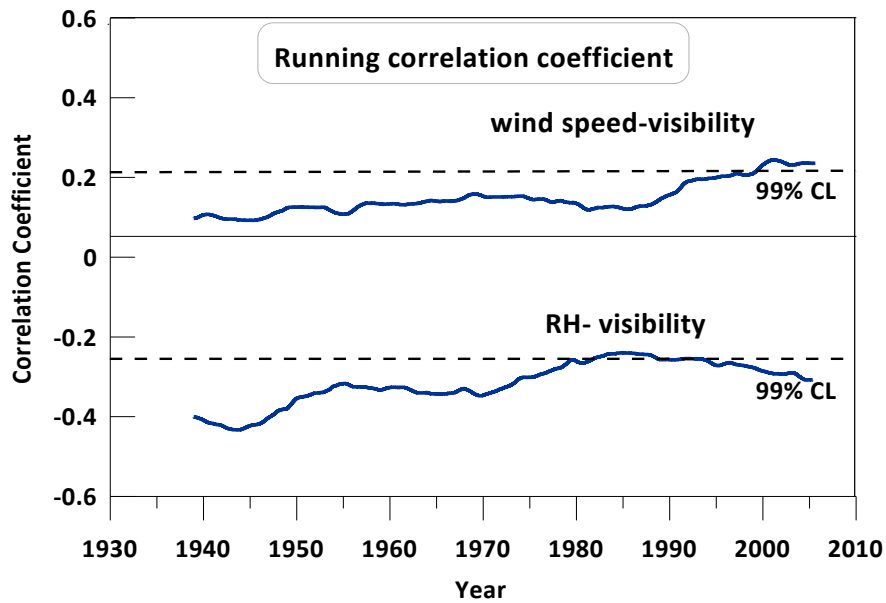


Fig.9. Running correlation coefficient and confidence levels between visibility and wind speed (up) and visibility and RH (bottom) in Athens, over the period 1931-2013. A 15-yr window was used.

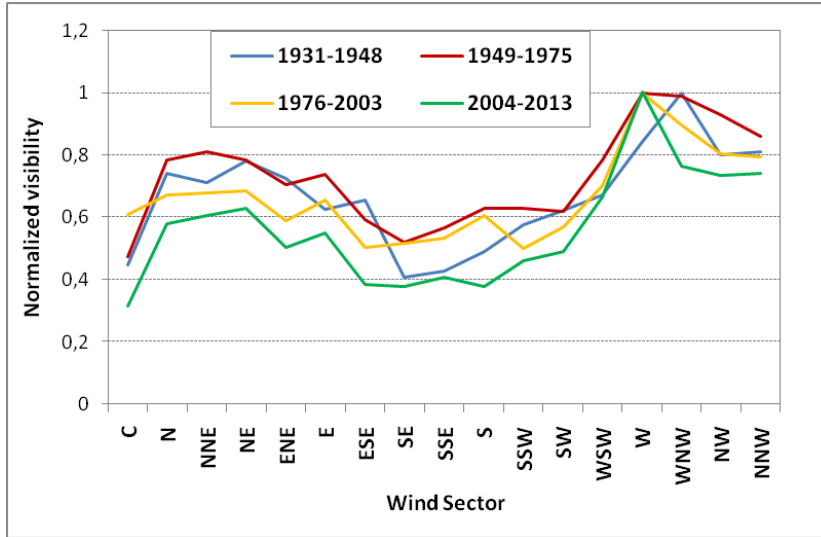


Fig. 10. Variation of visibility with wind direction (sectors) over the sub-periods 1931-1948, 1949-1975, 1976-2003 and 2004-2013. Visibility is normalized by its maximum value at a certain sector for each sub-period. Sector ‘C’ corresponds to calms (wind speed <math>< 0.3 \text{ m s}^{-1}</math>). Frequency of each sector approximates closely its climatic value (Fig. 3) in all sub-periods.

1053
1054
1055
1056
1057
1058
1059
1060
1061
1062
1063
1064
1065
1066
1067
1068
1069
1070
1071
1072
1073
1074
1075

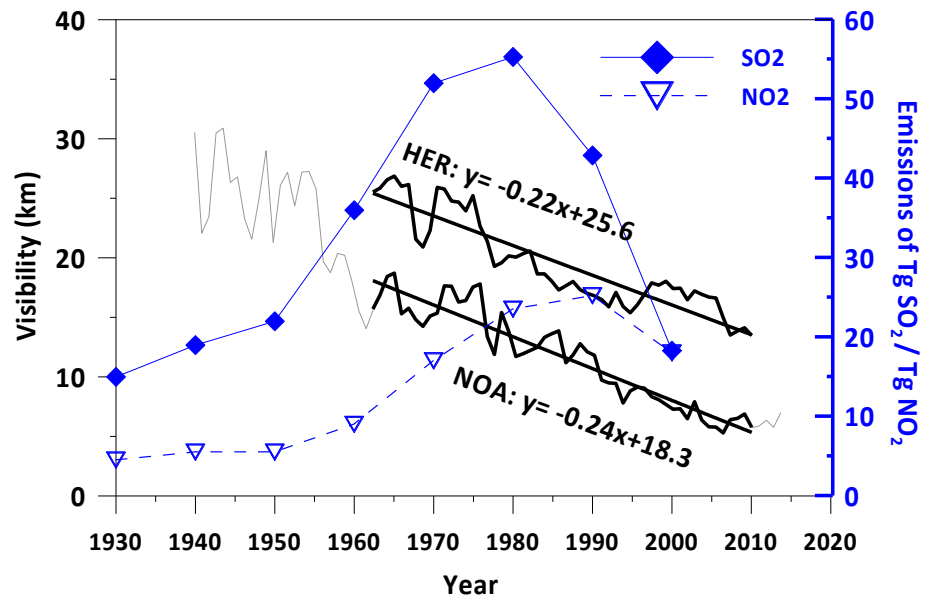


Fig. 11. Inter-decadal variability of the annual visibility at NOA (urban) and HER (background)stations. Bold black lines represent the common period of observations (1956-2009) at the two stations, along with linear trends and slopes. Solid blue line illustrates historical development of European emissions of SO₂, as included in Vestreng et al. (2007), and blue dashed line illustrates historical European emissions of NO_x, as included in Vestreng et al., 2009.

1076

1077

1078

1079

1080 **Fig. 12.** a) Variability of de-seasonalized monthly AVHRR-based AOD_{630nm} from 1981 to 2009 (black), along
 1081 with linear trends for the periods 1981-1997 (blue) and 1998-2009 (green). Vertical bars describe the standard
 1082 deviation of the annual value based on the monthly ones (upper graph).b) Variability of MODIS-based de-
 1083 seasonalized monthly AOD_{550nm} from 2000 to 2014 (red), along with lineartrends for the periods 2000-2009
 1084 (blue) and 2010-2014 (green). Vertical bars describe the standard deviation of the annual value based on the
 1085 monthly ones and grey horizontal bars the respective year (lower graph).

1086

1087

43

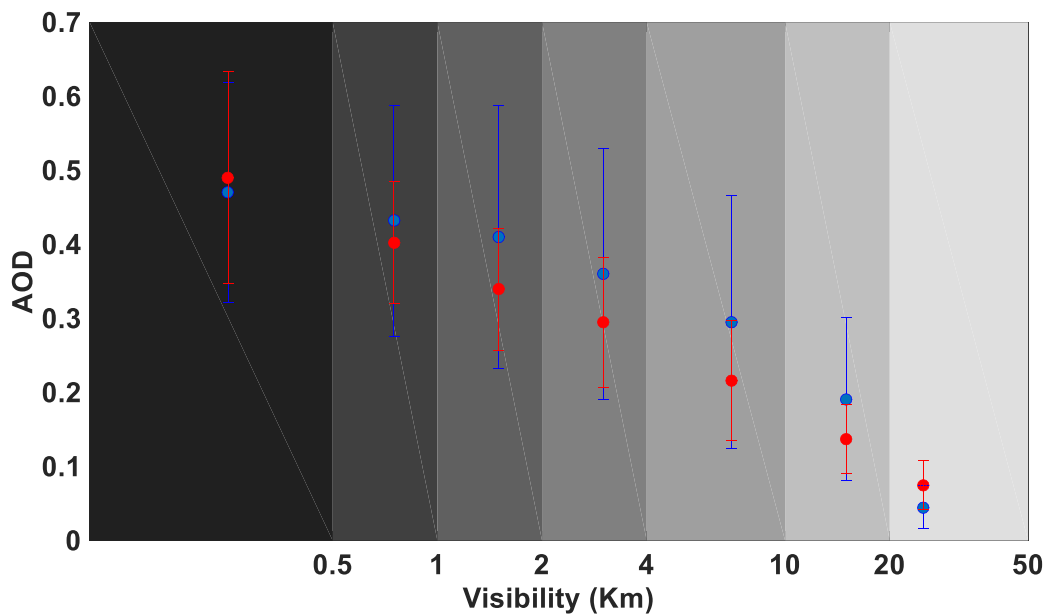
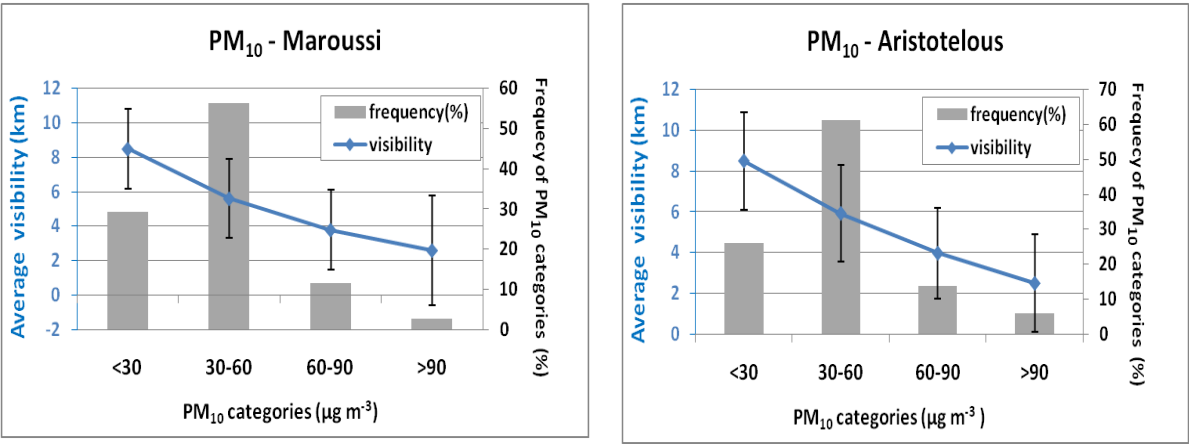


Fig.13. MODIS at 550nm (blue) (2000-2014) and AVHRR at 630nm (red) (1981-2009), AOD (June-August) mean values and standard deviations, for each visibility index. Shaded areas represent visibility ranges (km) for each visibility class (Table 2). AOD averages have been represented here in the average distance from each class.

1104
1105
1106



1107
1108
1109
1110
1111
1112
1113
1114
1115
1116
1117
1118

Fig. 14. Visibility as a function of different classes of PM₁₀ levels at an urban (Aristotelous) and a suburban (Maroussi) station in Athens. Measurements refer to the period 2008-2012. Geometric average and standard deviation are applied on visibility observations. Frequencies of different PM₁₀ classes are also shown (grey bars).

1119
1120
1121
1122
1123
1124
1125
1126
1127
1128
1129
1130
1131
1132
1133
1134

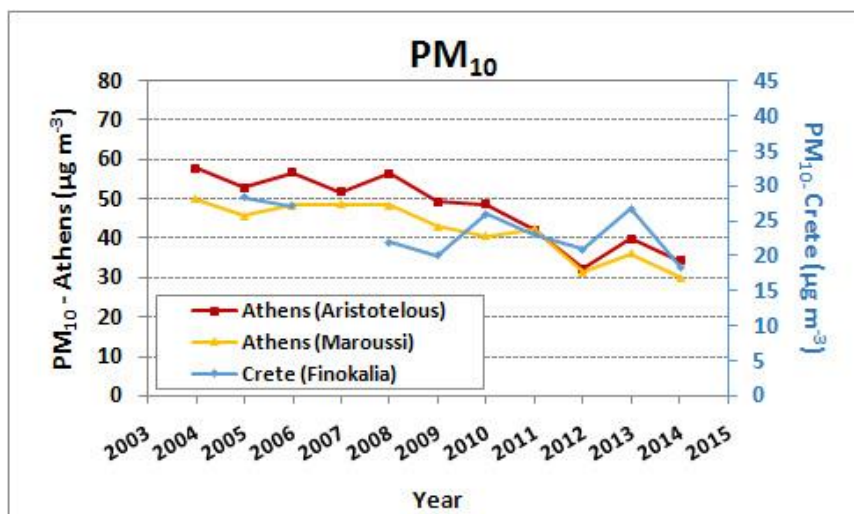


Fig. 15. Variation of the annual PM₁₀ levels at the reference station of Finokalia (2005-2014) and at the stations of Maroussi and Aristotelous in Athens (2004-2014).